buildings

MDPI

Article

Properties of Slag-Fly Ash Blended Geopolymer Concrete Reinforced with Hybrid Glass Fibers

Mohammad Zuaiter, Hilal El-Hassan *, Tamer El-Maaddawy and Bilal El-Ariss

Department of Civil & Environmental Engineering, United Arab Emirates University, Al-Ain P.O. Box 15551, United Arab Emirates; 201970258@uaeu.ac.ae (M.Z.); tamer.maaddawy@uaeu.ac.ae (T.E.-M.); bilal.elariss@uaeu.ac.ae (B.E.-A.)
* Correspondence: helhassan@uaeu.ac.ae

Abstract: Geopolymer concrete is typically characterized by a brittle behavior and limited crack resistance. This study evaluates the performance of ambient-cured slag-fly ash blended geopolymer concrete reinforced with glass fibers. Two types of glass fibers were used exclusively or as a hybrid combination. The workability of glass fiber-reinforced geopolymer concrete was assessed using the slump, compaction factor, and vebe time. The compressive strength, splitting tensile strength, and modulus of elasticity were used to characterize the mechanical properties, while water absorption, sorptivity, abrasion resistance, and ultrasonic pulse velocity were employed in evaluating the durability. Experimental results showed that the slump and compaction factor decreased by up to 75% and 18%, respectively, with glass fiber addition but less significantly in mixes reinforced with hybrid fiber combinations. Meanwhile, the vebe time increased by up to 43%. Hybrid glass fibers led to superior mechanical and durability properties compared to plain mixes and those reinforced with a single type of glass fiber, even at higher volume fractions. The compressive strength, splitting tensile strength, and modulus of elasticity increased by up to 77%, 60%, and 85%, respectively. While the water absorption decreased by up to 42%, the sorptivity, abrasion resistance, and ultrasonic pulse velocity increased by up to 67%, 38%, and 280%, respectively. Analytical regression models were established to predict the mechanical and durability characteristics of glass fiber-reinforced slag-fly ash blended geopolymer concrete and were compared to those of design codes.

Keywords: geopolymer; fly ash; slag; glass fibers; performance evaluation; hybrid; analytical models

Citation: Zuaiter, M.; El-Hassan, H.; El-Maaddawy, T.; El-Ariss, B. Properties of Slag-Fly Ash Blended Geopolymer Concrete Reinforced with Hybrid Glass Fibers. *Buildings* **2022**, *12*, 1114. https://doi.org/10.3390/buildings12081114

Academic Editors: Ahmed Senouci and Walid Maherzi

Received: 7 July 2022
Accepted: 25 July 2022
Published: 28 July 2022

1. Introduction

The consumption rate of concrete continues to increase, making it one of the most expended construction materials globally. Concrete and its main component, cement, are produced through the consumption of non-renewable natural resources and the emission of greenhouse gases. The increasing demand for urban development will result in a gradual increase in the consumption rate of concrete and, consequently, cement. According to cement statistics [1], the production of cement reached around 3.27 billion metric tons in 2020 and is expected to increase to 4.4 billion metric tons in the next ten years. China, India, and the United States account for annual cement production of 2.2 billion, 320 million, and 102 million metric tons, respectively [2]. Such wide utilization of cement in concrete could have an adverse long-term environmental impact. The production of 1 ton of cement emits nearly an equal amount of carbon dioxide (CO_2), thus contributing to 5–7% of the total global CO_2 emissions [3,4]. Nevertheless, the total anthropogenic CO_2 emissions from cement production could reach 10% in the near future. The emitted CO_2, among other greenhouse gases, is trapped in the atmosphere, resulting in an increase in global warming and subsequent occurrence of natural disasters, such as storms, heatwaves, floods, and droughts [5,6].

Several studies have addressed the utilization of supplementary materials in concrete, such as fly ash, granulated blast furnace slag, silica fume, rice husk ash, and metakaolin,

among others, as a partial replacement of cement in concrete to tackle its detrimental environmental impact. However, the complete replacement of cement is a more sustainable solution. Geopolymer technology is a promising technique to fully replace cement as the sole binder in concrete. Geopolymer binders are formulated through the combination of aluminosilicate materials and an alkaline activator solution. The properties of a geopolymer binder mainly depend on the characteristics of the aluminosilicate used, the composition of the alkaline activator, and the curing regime adopted [7–13]. Compared to cementitious binders, geopolymers have presented superior performance, including higher acid and fire resistance, better bond, lower alkali-aggregate expansion, and improved sulfate and corrosion resistance [2,14–17]. However, one of its major drawbacks is that it has lower resistance to cracking and high brittleness, exceeding that of conventional cement-based concrete [18].

The inclusion of fiber reinforcement in geopolymer concrete promises to improve its overall performance significantly and alleviate its drawbacks, i.e., brittle behavior and limited crack resistance. Carbon fibers (CF) have shown to improve the mechanical properties of geopolymer composites, including compressive strength, impact resistance, hardness, toughness, elastic modulus, and flexural strength [19–22]. Furthermore, steel fibers (SF) have been used on several occasions [23]. Medljy et al. [23] investigated the effect of SF inclusion on the mechanical properties of alkali-activated slag-fly ash blended concrete. It was concluded that the addition of SF had an adverse effect on the workability but a significant enhancement in the mechanical properties and durability. Few studies have investigated the effect of utilizing a hybrid combination of fibers. In two studies, the performance of slag-fly ash blended geopolymer was enhanced by utilizing single and hybrid SF [24,25]. Results revealed that hybridization of SF up to a certain dosage led to superior mechanical properties compared to those with a single type of fiber.

While various studies have focused on utilizing SF in geopolymer concrete, others have evaluated the effect of other types of fibers on the performance of geopolymer concrete. Several research works have focused on utilizing glass fibers (GF) in fly ash based geopolymer concrete [26–30]. Kumar et al. [28] evaluated the effect of SF and GF on the mechanical performance of geopolymer concrete. It was revealed that increasing the amount of GF enhanced the mechanical properties but to a lesser extent than SF. Lakshmi and Rao [29] evaluated the properties of fly ash based geopolymer concrete incorporating GF. Results showed that the addition of GF of up to 3%, by volume, enhanced the mechanical properties. However, a further increase in GF volume fraction resulted in a reduction in strength. In another work, the addition of GF decreased the geopolymer concrete workability, enhanced its mechanical properties, and slightly improved its durability [28,29]. Furthermore, Vijai et al. [30] investigated the effect of GF on slag-fly ash cement blended geopolymer concrete. Results revealed that the addition of 0.03% GF volume fraction led to superior strengths. Summarizing the literature, it is clear that GF have the potential to improve the properties of geopolymer concrete. However, it seems that the effect of GF on the mechanical and durability properties of a geopolymer concrete made with slag and fly ash has not been examined. In addition, the impact of hybridizing GF has not been evaluated.

Accordingly, this paper aims to evaluate the fresh and hardened properties of slag-fly ash blended geopolymer concrete reinforced with GF. Two different types of GF were used, namely 24 and 43 mm long (A and B) at three volume fractions (0.5%, 1.0%, and 1.5%). The two types of GF were added into the geopolymer concrete mix either exclusively or in a hybrid combination with A-to-B ratios of 3:1, 1:1, and 1:3 and at a volume fraction of 1.0%. Slag and fly ash were blended in a 3:1 ratio to form the binding material to eliminate the need for heat curing and reduce shrinkage cracks associated with fly ash- and slag-based geopolymers, respectively. The slump, compaction factor, vebe time, compressive strength, splitting tensile strength, modulus of elasticity, water absorption, sorptivity, abrasion resistance, and ultrasonic pulse velocity were employed in evaluating the performance of the geopolymer concrete. Analytical regression models were proposed to correlate the mechanical and durability properties among each other and were compared to those

developed in past literature and design codes. This work provides novel fundamental data on the material characteristics that are essential for industry practitioners and researchers to understand the behavior of slag-fly ash blended geopolymer concrete structures reinforced with single and hybrid glass fibers.

2. Materials and Methods

2.1. Materials

The geopolymer binding materials included ground granulated blast furnace slag (referred to hereafter as slag) and fly ash. The slag was locally sourced from Emirates Cement Company, Al Ain, United Arab Emirates, while the fly ash was from Ashtech Ltd, Abu Dhabi, United Arab Emirates. Table 1 summarizes the chemical composition of the as-received materials. Slag was mainly composed of calcium oxide (CaO) and silica (SiO_2), while fly ash was made of silica (SiO_2) and alumina (Al_2O_3). Their physical appearance is illustrated in Figure 1. The morphologies of the as-received binding materials were obtained through a JEOL JSM 6390A scanning electron microscopy (SEM), Tokyo, Japan, as shown in Figure 2. Furthermore, the main components present in slag and fly ash were quartz and mullite, as illustrated in the X-ray diffraction (XRD) spectra presented in Figure 3 and obtained using a Malvern Panalytical XRD, Malvern, United Kingdom. Their gradation curves, depicted in Figure 4, show that the particle sizes of slag and fly ash were in the ranges of 2–80 and 0.2–40 μm.

Table 1. Chemical composition and physical properties of the as-received materials.

Oxide Compound	Material (%)		
	Slag	**Fly Ash**	**Dune Sand**
CaO	42.0	3.3	14.1
SiO_2	34.7	48.0	64.9
Al_2O_3	14.4	23.1	3.0
MgO	6.9	1.5	1.3
Fe_2O_3	0.8	12.5	0.7
Loss in ignition	1.1	1.1	0.0
Others	1.1	10.5	16.0
Physical Properties			
Blaine fineness (cm^2/g)	4250	3680	117
Uniformity coefficient	2.86	9.10	1.47
Curvature coefficient	0.71	1.45	1.09
Specific gravity	2.70	2.32	2.77

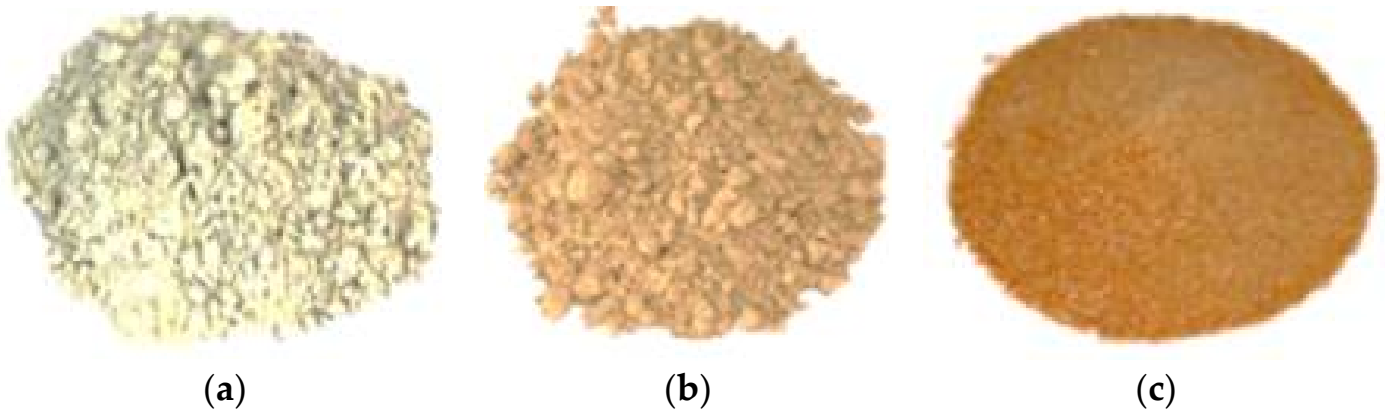

Figure 1. Physical appearance of (**a**) slag, (**b**) fly ash, and (**c**) dune sand.

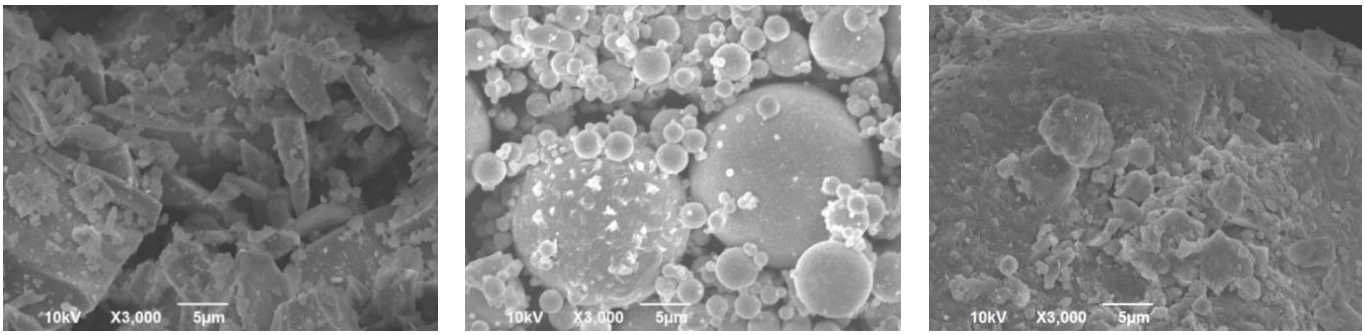

(**a**) (**b**) (**c**)

Figure 2. SEM micrographs of (**a**) slag, (**b**) fly ash, and (**c**) dune sand.

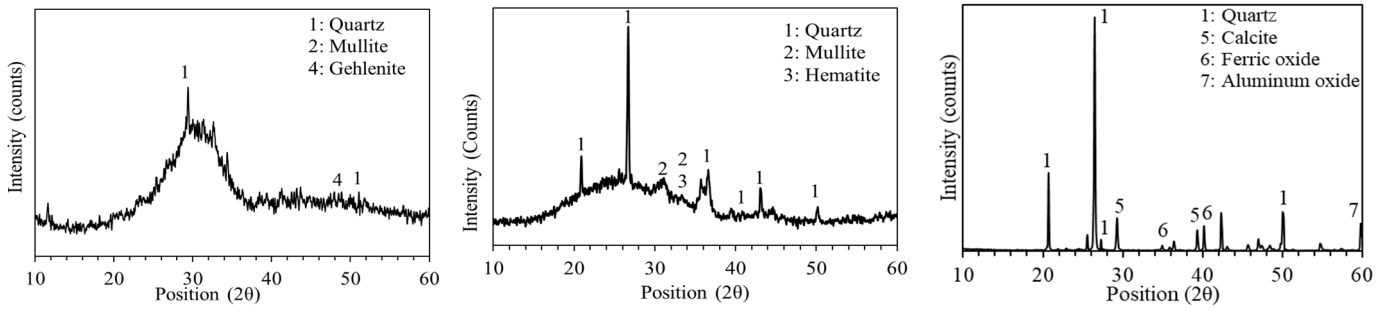

(**a**) (**b**) (**c**)

Figure 3. XRD spectrum of (**a**) slag, (**b**) fly ash, and (**c**) dune sand.

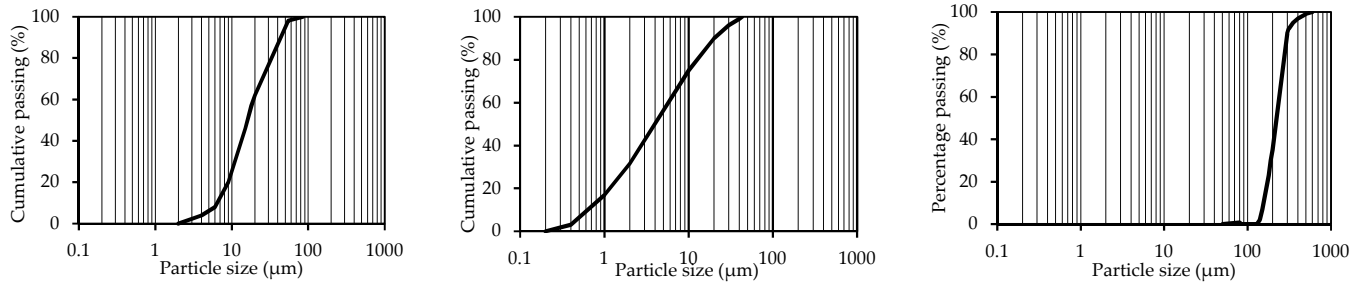

(**a**) (**b**) (**c**)

Figure 4. Particle size distribution of (**a**) slag, (**b**) fly ash, and (**c**) dune sand.

Dune sand (Figure 1c) served as the fine aggregates in the geopolymer concrete mixes. Its morphology, phase analysis, and particle size distribution, shown in Figures 2c, 3c and 4c, respectively, highlight the predominant presence of SiO_2 in the form of angular particles. As shown in Table 1, it is characterized by a specific surface area of 117 cm^2/g and specific gravity of 2.77. Furthermore, natural crushed dolomitic limestone aggregates (NA), with an NMS of 20 mm, were used as coarse aggregates. Their physical properties are presented in Table 2. It is composed of 59% CaO, 32% MgO, 6% SiO_2, 1.6% Al_2O_3, and 1.4% other oxide compounds.

The alkaline activator solution was formulated by mixing sodium silicate (SS) and sodium hydroxide (SH). The SS solution was grade N with a chemical composition of 26.3% SiO_2, 10.3% Na_2O, and 63.4% H_2O. The SH solution was prepared by dissolving 97% of pure SH flakes in a specific amount of water to attain molarity of 14 M, as recommended in another work [35,36]. Furthermore, to maintain adequate fresh workability of the geopolymer concrete, a polycarboxylic ether-based polymer-based superplasticizer (SP) and additional water were incorporated into the mix. Two types of alkali-resistant glass

fibers (GF) were used, Type A and B, as shown in Figure 5. They were sourced from ReforceTech [37]. Their physical properties, summarized in Table 3, feature a similar diameter, Young's modulus, specific gravity, and tensile strength, while their length and aspect ratio were different. In this work, the use of the two types of fibers served to investigate the effect of fiber length on the properties of slag-fly ash blended geopolymer concrete.

Table 2. Physical properties of natural aggregates (NA).

Physical Property, Unit	Standard Test	Value
Fineness modulus	[31]	6.82
Water absorption, %	[32]	0.20
Specific gravity	[33]	2.82
Dry-rodded density, kg/m^3	[33]	1635
Los Angeles abrasion, %	[34]	16.0
Specific surface area, cm^2/g	[31]	2.49
Soundness ($MgSO_4$), %	[34]	1.20

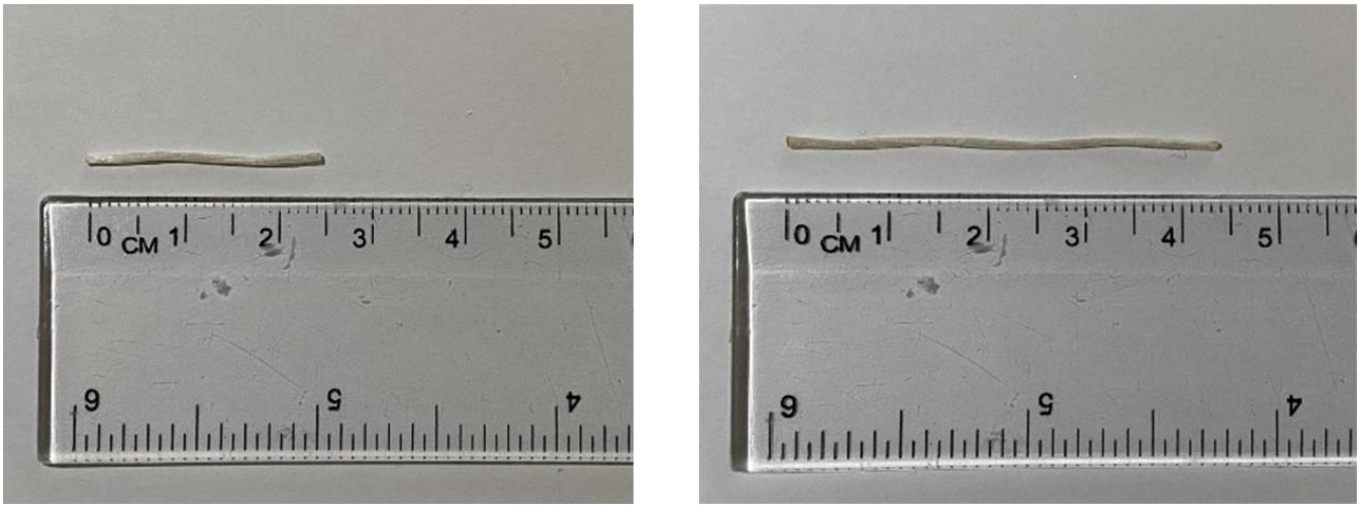

(**a**) (**b**)

Figure 5. Glass fibers with lengths of (**a**) 24 and (**b**) 43 mm.

Table 3. Properties of the glass fibers.

Property, Unit	Type A	Type B
Length, mm	24	43
Diameter, mm	0.7	0.7
Aspect ratio	35	62
Tensile strength, MPa	>1000	>1000
Young's modulus, GPa	42	42
Specific gravity	2.0	2.0

2.2. Mixture Proportioning

The mixture proportions of the geopolymer concrete mixes are presented in Table 4. The control mix (A0B0GF0.0) was designed to attain a cube compressive strength (f_{cu}) of 30 MPa and a slump of 150 mm. The remaining mixes had similar proportions to the control mix while varying the GF volume fraction, type, and combinations. The total binder consisted of slag and fly ash blended at a 3:1 ratio. Previous work reported that this blend possessed superior performance over others, owing to the coexistence of calcium aluminosilicate hydrate (C-A-S-H) and sodium aluminosilicate hydrate (N-A-S-H) gels [2,15,35]. Furthermore, such a blend is intended to eliminate the heat curing associated

with fly ash based geopolymer and reduce shrinkage that occurs from the alkali-activated slag concrete. Dune sand content, coarse aggregates content, SS-to-SH ratio, SH molarity, and SP content were fixed for all mixes at 725 kg/m^3, 1210 kg/m^3, 1.5, 14 M, and 7.5 kg/m^3 (2.5% of binder mass), respectively. The additional water content of 75 kg/m^3 was added to all mixes to enhance the workability, as recommended in past studies [38–41]. Two types of GF, Type A and B, were utilized in the geopolymer concrete mixes at various volume fractions, including 0.5%, 1.0%, and 1.5%. Hybrid combinations of GF, consisting of blends of both types of GF (A and B), were utilized in the mix at a volume fraction of 1%. Three different A:B ratios were explored, namely 3:1, 1:1, and 1:3. Preliminary test results showed that mixes made with a hybrid GF combination 1:1 at a volume fraction of 1.0% had similar compressive and splitting tensile strengths as counterparts made with 1.5% GF, by volume. However, the latter had significantly lower workability. For this reason, a volume fraction of 1% was selected for hybrid mixes.

Table 4. Mixture proportions of geopolymer concrete mixes (kg/m^3).

Group	Mix Designation	Binder		Dune Sand	Coarse Aggregates	AAS		SP	Water	Glass Fibers	
		Slag	Fly Ash			SS	SH			Proportions (A:B)	v_f (%)
Control	A0B0GF0.0.0	225	75	725	1210	99	66	7.5	75	0:0	0.0
A	A100B0GF0.5	225	75	725	1210	99	66	7.5	75	1:0	0.5
	A100B0GF1.0	225	75	725	1210	99	66	7.5	75	1:0	1.0
	A100B0GF1.5	225	75	725	1210	99	66	7.5	75	1:0	1.5
B	A0B100GF0.5	225	75	725	1210	99	66	7.5	75	0:1	0.5
	A0B100GF1.0	225	75	725	1210	99	66	7.5	75	0:1	1.0
	A0B100GF0.5	225	75	725	1210	99	66	7.5	75	0:1	1.5
C	A25B75GF1.0	225	75	725	1210	99	66	7.5	75	3:1	1.0
	A50B50GF1.0	225	75	725	1210	99	66	7.5	75	1:1	1.0
	A75B25GF1.0	225	75	725	1210	99	66	7.5	75	1:3	1.0

2.3. Sample Preparation

The geopolymer concrete mixes were prepared and cast under ambient laboratory conditions with a temperature and relative humidity of 23 ± 2 °C and 50 ± 5%, respectively. At first, the SH flakes were mixed with a specific amount of water to attain an SH solution molarity of 14 M. After the SH solution reached room temperature, the SS was mixed with the SH solution. The heat generated from the newly formed AAS was allowed to dissipate overnight. The AAS was then mixed with the additional water and SP prior to casting and gradually poured onto the dry ingredients, i.e., slag, fly ash, coarse aggregates, and dune sand, and mixed for an additional three minutes to attain a homogeneous and uniform concrete mix. Subsequently, the fresh geopolymer concrete was cast into 100 mm cubes and 100 × 200 mm (diameter × height) cylinders and compact-vibrated on a vibrating table for a duration of 10 s. The geopolymer samples were then covered with a plastic sheet for 24 h, demolded, and left at ambient conditions until testing age. Figure 6 shows the casting procedure.

Figure 6. Casting of geopolymer concrete samples.

2.4. Performance Evaluation

2.4.1. Fresh and Physical Properties

The slump test was carried out to evaluate the effect of different GF types, volume fractions, and combinations on the workability of the slag-fly ash blended geopolymer concrete mixes. It was conducted on fresh concrete in accordance with ASTM C143 [42]. In addition, the fresh and 28-day hardened concrete densities were determined according to ASTM C138 [43] and ASTM C642 [44], respectively.

The compactability of slag-fly ash blended geopolymer concrete was evaluated through a compaction factor test, in accordance with BS 1993: Part 103 [45]. Fresh concrete was allowed to pass through two conical hoppers under its own weight, after which it was dropped into a cylindrical mold. The weight of the cylinder filled with concrete was measured (i.e., uncompacted mass). Subsequently, the cylinder was compact-vibrated on a vibrating table and weighed again (i.e., compacted mass). The compaction factor is the ratio of the uncompacted mass of the cylinder to its compacted mass. The higher the compaction factor, the better the compactability of the mix.

The behavior of fresh slag-fly ash blended geopolymer concrete during vibration was evaluated by the vebe time test. The test was conducted in accordance with BS EN 12350-1 [46], where the consistency of fresh concrete was measured in seconds. The time needed for the plate disc to be fully in contact with the concrete is considered as vebe time in seconds. The shorter the time taken, the more consistent the concrete mix.

2.4.2. Mechanical Properties

The cube (f_{cu}) and cylinder compressive strength (f'_c) of slag-fly ash blended geopolymer concrete was determined using a Wykeham Ferrance machine with a loading capacity of 2000 kN in accordance with BS EN 12390-3 [47] and ASTM C39 [48], respectively. An axial load was applied at a loading rate of 7 kN/sec. The cube compressive strengths of geopolymer concrete mixes were obtained at 1, 7, and 28 days, while the cylinder compressive strength was obtained at 28 days only. For each test, three samples were tested per mix to obtain an average. Figure 7a shows a geopolymer concrete specimen during compressive strength testing.

(**a**) (**b**)

Figure 7. Geopolymer concrete specimen during (**a**) compressive and (**b**) splitting tensile strength testing.

In addition, experimental stress–strain curves were developed to obtain the peak stress, peak strain, and modulus of elasticity E_c, according to ASTM C469 [49]. A compression load cell with 500 kN capacity was used to record the applied load. Two 60 mm long strain gauges were attached vertically at mid-height and diametrically opposite points of the cylinder circumference to record the axial strains. The load cell and strain gauges were connected to a data acquisition system to obtain the stress–strain response. The modulus of elasticity, E_c, was obtained as the slope of the chord connecting the stress corresponding to 40% of the ultimate stress (S_2) and the corresponding stress of a strain of 0.00005 (S_1). Equation (1) was employed in determining the modulus of elasticity of the glass fiber reinforced slag-fly ash blended geopolymer concrete mixes. The average of three samples was taken per mix to represent E_c.

$$E_c = \frac{S_2 - S_1}{\varepsilon_2 - 0.00005} \quad (1)$$

The splitting tensile strength (f_{sp}) of 28-day slag-fly ash blended geopolymer concrete was determined in accordance with ASTM C496 [50]. The load was applied across the entire length of the specimen at a loading rate of 1 kN/sec. Cylinders of 100 mm diameter and 200 mm height were used. Triplicate specimens were tested per mix to find the average, as shown in Figure 7b.

2.4.3. Durability Properties

The water absorption of 28-day concrete mixes was evaluated in accordance with ASTM C642 [44]. Concrete disc specimens of 100 mm diameter and 50 mm height were employed. The oven-dried mass was obtained by placing the specimen in an oven at 105 °C for 24 h until a mass change of less than 0.5% was achieved. Afterward, the oven-dried specimens were immersed in water for another 24 h, after which the saturated surface-dry (SSD) mass was recorded. Triplicate samples were tested per mix. The water absorption was calculated using Equation (2).

$$\text{Water absorption } (\%) = \frac{\text{SSD mass (g)} - \text{Oven-dry mass (g)}}{\text{Oven-dry mass (g)}} \times 100\% \quad (2)$$

The rate of absorption, i.e., sorptivity, was measured on 28-day disc specimens, similar to those used in the water absorption test, as per ASTM C1585 [51]. Three specimens were tested for each mix to find the average. The circumference of the top surface of the specimen was sealed with adhesive tape to allow water to penetrate from the bottom side only and to avoid evaporation. The mass of the disc concrete specimens was recorded at 1, 5, 10, 15, 20, 30, and 60 min and after every hour up to 6 h. The rate of absorption was obtained using Equation (3). The absorption rate against the square root of time was plotted, and the slope of the best-fit line was identified as the initial rate of water absorption ($mm/s^{0.5}$), i.e., sorptivity.

$$\text{Rate of Absorption, I (mm)} = \frac{\text{Change in mass at time t (g)}}{\text{Exposed area (mm}^2\text{)} \times \text{density of water } \left(\text{g/mm}^3\right)} \quad (3)$$

The resistance of 28-day slag-fly ash blended geopolymer concrete to friction and abrasive actions was evaluated using the Los Angeles (LA) abrasion test. This is an indicative measure of the durability of so-produced concrete [52]. The test was conducted according to the procedure of ASTM C1747 [53]. Three replicates of disc specimens of 100 mm diameter and 50 mm height were tested. The mass of the disc specimen was recorded prior the starting the test and after every 100 revolutions up to 500 revolutions. Equation (4) was used in obtaining the mass loss of samples.

$$\text{Mass Loss (\%)} = \frac{\text{Final Mass} - \text{Initial Mass}}{\text{Initial Mass}} \times 100\% \quad (4)$$

The uniformity and relative quality of the concrete were assessed through a non-destructive ultrasonic pulse velocity (UPV) test. The test was performed in accordance with ASTM C597 [54]. A total of three cube concrete specimens per mix were subjected to UPV to obtain an average transit time in seconds. The electro-acoustical transducer generates longitudinal pulses that are then received by a second transducer located at a distance, L, from the transmitting transducer. The time in seconds was obtained from the device, and Equation (5) was used in calculating the velocity.

$$\text{Velocity (m/s)} = \frac{\text{L (m)}}{\text{Time (s)}} \times 100\% \quad (5)$$

3. Experimental Results and Discussion

3.1. Slump

The slump test was used to evaluate the workability of slag-fly ash blended geopolymer concrete incorporating different types (A or B), volume fractions (0.5, 1.0, and 1.5%), and combinations (single or hybrid) of GF. The slump values, presented in Table 5, ranged between 40 and 160 mm, with the highest workability being for the plain geopolymer concrete mix (A0B0GF0.0). The addition of GF reduced the workability in geopolymer mixes. A similar outcome was reported when adding glass fibers to fly ash based geopolymer concrete [29,55,56].

Table 5. Slump, compaction factor, and vebe time for geopolymer concrete mixes.

Mix Designation	Slump (mm)	Change in Slump (%) *	Compaction Factor	Change in Compaction Factor (%) *	Vebe Time (sec)	Change in Vebe Time (%) *
A0B0GF0.0	160	-	0.94	-	3.5	-
A100B0GF0.5	85	−46.8	0.92	−2.1	3.6	2.9
A100B0GF1.0	80	−50.0	0.90	−4.3	3.7	5.7
A100B0GF1.5	50	−68.7	0.87	−7.5	4.6	31.4
A0B100GF0.5	75	−53.1	0.86	−8.5	4.0	14.3
A0B100GF1.0	50	−68.7	0.80	−14.9	4.6	31.4
A0B100GF1.5	40	−75.0	0.77	−18.1	5.0	42.9
A75B25GF1.0	110	−31.2	0.91	−3.2	3.6	2.9
A50B50GF1.0	100	−37.5	0.88	−6.4	4.2	20.0
A25B75GF1.0	55	−65.6	0.78	−17.0	4.7	34.3

* With respect to the control mix A0B0GF0.0.

Series A mixes, incorporating type A (24 mm long) GF at 0.5%, 1.0%, and 1.5% volume fractions, exhibited slump reductions of 47%, 50%, and 69%, respectively. Conversely, series B mixes, incorporating type B (43 mm long) GF at similar volume fractions, resulted in further reductions in the slump of 53%, 69%, and 75%, respectively. Apparently, the incorporation of longer GF (type B) was more impactful on the workability of slag-fly ash blended geopolymer concrete. To accommodate for such loss in workability, an additional amount of paste would be required to cover the longer glass fibers and further enhance the workability. Additionally, the reduction in the slump was more evident when increasing the glass fiber volume fraction, i.e., 1.5%, as increasing the fiber content in the mix increased the probability of fiber overlap and agglomeration. A similar phenomenon was noted in other studies on fly ash and silica fume blended geopolymer concrete mixes [57]. Meanwhile, it is possible to incorporate a higher volume fraction of short GF (type A) than long GF (type B) while attaining similar workability. For example, A100B0GF1.5 and A0B100GF1.0 mixes resulted in a similar slump.

Hybrid combinations of both GF types (A and B) at a constant volume fraction of 1% were incorporated in series C mixes. Short GF were replaced with long GF at replacement percentages of 25%, 50%, and 75%. Replacing 25% of short GF with longer ones, i.e., A75B25GF1.0, increased the slump by 30 mm (i.e., 38%) compared to its counterpart mix made with 100% short fibers, i.e., A100B0GF1.0. Further increases in the replacement percentage by 50% and 75% decreased the slump by 10 and 55 mm in comparison with the mix at 25% replacement, respectively. However, mixes with a hybrid combination of GF resulted in a better slump than its counterpart mix A0B100GF1.0. This is owed to the reduction of the fiber interlocking effect and cross-linking ability. A similar phenomenon was noted when the length of polyethylene fiber was increased in fly ash, slag, and silica fume based geopolymer concrete [57].

3.2. Compaction Factor

The compaction factor test results were consistent with those of the slump test. The plain control mix resulted in the highest compaction factor of 0.94. In comparison, the incorporation of short GF by 0.5%, 1.0%, and 1.5%, by volume, decreased the compaction factor by 2%, 4%, and 7%, respectively. Meanwhile, the inclusion of long GF at similar volume fractions decreased the compaction factors by 7%, 15%, and 18%, respectively, with reference to the control mix. A higher loss in compactability was noted when the long GF (type B) volume fraction increased from 0.5% to 1.0%, while a milder decrease was observed when the volume fraction further increased to 1.5%. It is possible to incorporate more type A than type B GF while experiencing similar compactability of geopolymer concrete. Such a finding is owed to the higher probability of fiber interlocking effect that occurs in mixes with longer fibers [56–59].

Mixes with hybrid GF combination at 1% volume fraction decreased the compaction factors but to a lesser extent than those of mixes with long glass fibers. Replacing 25% of short glass fibers with long ones (A75B25GF1.0) had an insignificant impact on the compactability of geopolymer concrete mix compared to the plain control mix (A0B0GF0.0).

Further increases in replacement percentages by 50% and 75% resulted in compaction factors of 0.88 and 0.78, representing 6% and 17% losses in compactability compared to the control mix, respectively. Evidently, the addition of a hybrid GF combination with long GF content of 75–100% of the total fiber volume had a more detrimental effect on the compactability. Such decreases in compactability are attributed to mixes with slump values less than 55 mm.

3.3. Vebe Time

The vebe times for plain and glass fiber-reinforced slag-fly ash blended geopolymer concrete are presented in Table 5. The plain control mix had a vebe time of 3.5 s, while those of mixes of series A and B resulted in vebe times in the ranges of 3.6–4.6 s and 4.0–5.0 s, respectively. The inclusion of 0.5% and 1.0% short GF, by volume, caused insignificant increases in the vebe time of 3% and 6%, respectively. Conversely, the smallest addition of type B GF, i.e., 0.5%, by volume, resulted in a 14% increase in the vebe time. This highlights a more significant impact of long GF on the cohesiveness of geopolymer concrete than their short counterparts. Further increases in either type of GF increased the vebe time. Similar outcomes were reported in steel fiber-reinforced cement-based concrete [58]. Nevertheless, A100B0GF1.5 and A0B100GF1.0 had similar vebe times despite the mix with short fibers having a higher GF volume fraction.

In hybrid mixes of series C, the replacement of short with long GF by 25%, 50%, and 75% at a constant volume fraction of 1% resulted in vebe times of 3.6, 4.2, and 4.6 s, respectively. An increase in vebe time was noted when increasing the amount of long GF in a hybrid combination, indicating a reduction in the cohesiveness of the mix. Their counterpart non-hybrid mixes, i.e., at 1% volume fraction, in series A and B, resulted in vebe times of 3.7 and 4.6 s, respectively. Hence, replacing 25% of type A with type B had no impact on the vebe time, after which the vebe time increased. Moreover, mixes with 75–100% replacement percentages of short with long GF resulted in similar vebe times. This is due to the higher interlocking effect associated with long GF, as noted in past studies with other types of fibers [56–59]. These relatively longer vebe times are associated with compaction factors and slump of at most 0.8 and 55 mm.

3.4. Fresh and Hardened Density

The fresh and 28-day hardened densities are presented in Table 6. The values for the fresh and hardened density were in the respective ranges of 2509–3205 and 2303–2554 kg/m^3. Evidently, the addition of GF increased the fresh and hardened densities of slag-fly ash blended geopolymer concrete. Further increases were noted when increasing the GF volume fraction. The addition of 0.5%, 1.0%, and 1.5% of short GF resulted in 10%, 12%, and 23% higher fresh densities compared to the control mix, respectively. Meanwhile, the inclusion of long GF at similar volume fractions led to 13%, 14%, and 24% respective increases. Moreover, adding either type of fiber at 0.5%, 1.0%, and 1.5% volume fractions increased the 28-day hardened density by 5%, 6%, and 10%, respectively, with reference to the control mix. Such results highlight a relatively limited impact of fiber length on the fresh and 28-day hardened density of slag-fly ash blended geopolymer concrete.

Table 6. Fresh and hardened densities of geopolymer concrete mixes.

Mix ID	Fresh Density (kg/m^3)	Hardened Density (kg/m^3)
A0B0GF0.0	2509 ± 126	2303 ± 116
A100B0GF0.5	2765 ± 111	2410 ± 150
A100B0GF1.0	2808 ± 169	2422 ± 146
A100B0GF1.5	3084 ± 173	2541 ± 143
A0B100GF0.5	2845 ± 200	2414 ± 169
A0B100GF1.0	2915 ± 117	2439 ± 105
A0B100GF1.5	3110 ± 187	2543 ± 153
A75B25GF1.0	3039 ± 152	2545 ± 128
A50B50GF1.0	3131 ± 220	2550 ± 179
A25B75GF1.0	3205 ± 257	2554 ± 205

Replacing short GF with long ones in a hybrid combination by 25%, 50%, and 75% resulted in 21%, 25%, and 28% respective increases in fresh density, with reference to the control mix. Conversely, the hardened density increased by nearly 11% regardless of the hybrid GF combination. Furthermore, the difference between the fresh and hardened densities increased as the length of GF, the volume fraction of GF, and the ratio of long-to-short GF increased. This shows that the GF were more impactful on the fresh density than on the 28-day hardened density. Based on these results, a strong correlation between the two densities was developed with a coefficient R^2 of 0.96, as presented in Equation (6) and Figure 8. Such correlation makes it possible to predict the 28-day hardened concrete density (ρ_h) from the measured fresh concrete density (ρ_f) for slag-fly ash blended geopolymer concrete presented in this work.

$$\rho_h = 0.4\,\rho_f + 1305.4 \quad (6)$$

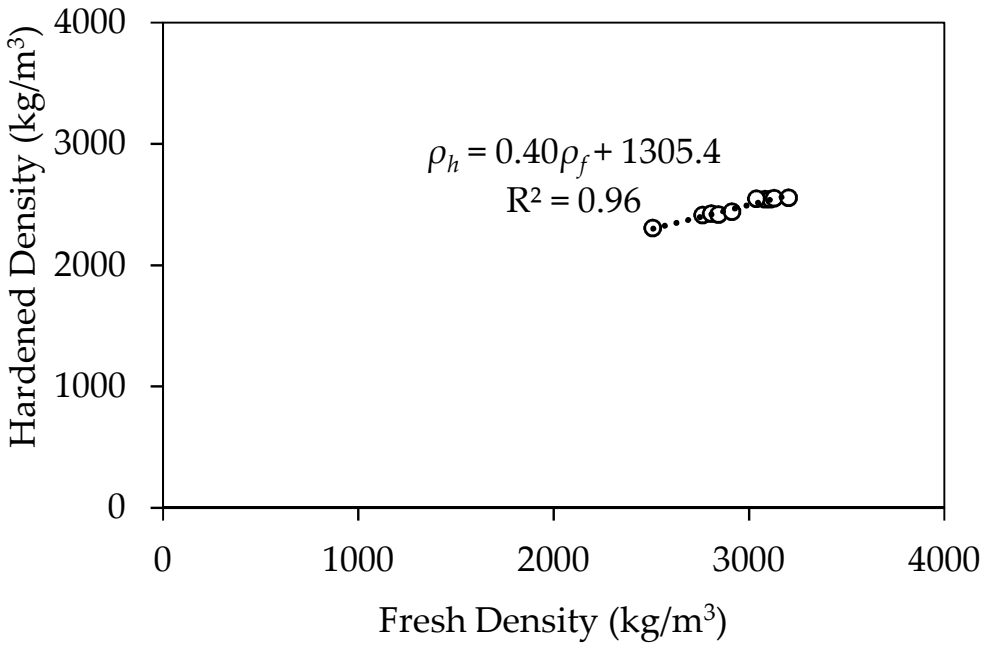

Figure 8. Relationship between fresh and hardened densities.

3.5. Compressive Strength

The 1-, 7-, and 28-day compressive strengths of slag-fly ash blended geopolymer concrete mixes with different types, volume fractions, and combinations of GF are summarized in Table 7. The values of f_{cu} at 1, 7, and 28 days were in the ranges of 23.2–32.4, 31.9–40.2, and 33.3–42.2 MPa, respectively, with the plain control mix (A0B0GF0.0) having the lowest strength at each age. Results showed that the incorporation of GF led to an increase in f_{cu}. Such a finding correlates well with the enhancement in the 28-day hardened density upon incorporating GF. For instance, the 1-day f_{cu} increased by 9%, 13%, and 24% upon the addition of 0.5%, 1.0%, and 1.5% short GF volume fractions, respectively. Meanwhile, the incorporation of the same short GF volume fractions resulted in 5%, 6%, and 17% higher 7-day f_{cu} and 11%, 13%, and 20% higher 28-day f_{cu}, respectively. The 1-, 7-, and 28-day f_{cu} resulted in average increases of 16%, 9%, and 16%, with the addition of 1.0% short GF, by volume. Similarly, the addition of long glass fibers enhanced the f_{cu} at all ages, with reference to the control mix. For every 1.0% long GF added, by volume, the 1-, 7-, and 28-day f_{cu} increased by, on average, 20%, 21%, and 18%, respectively. The addition of long GF was more impactful on f_{cu} at all ages than short GF, as longer fibers had a better bridging effect and ability to suspend crack formation and propagation [28–30].

Table 7. Results of compressive and tensile strengths and modulus of elasticity.

Mix Designation	Compressive Strength, f_{cu} (MPa)			Strength Development of f_{cu}		f'_c	f_{sp} (MPa)	f'_c/f_{cu}	f_{sp}/f'_c	E_c (GPa)
	1-Day	7-Day	28-Day	1d–7d (%) [a]	7d–28d (%) [b]					
A0B0GF0.0	23.2 ± 1.2	31.9 ± 0.9	33.3 ± 0.2	37.5	4.4	12.4 ± 1.2	2.2 ± 0.1	0.37	0.18	4.6 ± 0.2
A100B0GF0.5	25.4 ± 1.4	33.6 ± 0.9	36.9 ± 1.1	32.3	9.8	14.3 ± 2.1	2.6 ± 0.1	0.39	0.18	5.4 ± 0.2
A100B0GF1.0	26.2 ± 0.4	33.9 ± 1.1	37.5 ± 0.5	29.4	10.6	16.2 ± 1.5	2.8 ± 0.1	0.43	0.17	5.8 ± 0.2
A100B0GF1.5	28.7 ± 0.9	37.4 ± 0.8	39.9 ± 1.6	30.3	6.7	17.6 ± 3.2	2.9 ± 0.2	0.44	0.17	6.8 ± 0.3
A0B100GF0.5	25.8 ± 1.2	36.8 ± 3.1	37.4 ± 0.3	42.6	1.6	14.0 ± 0.9	2.6 ± 0.6	0.37	0.19	5.6 ± 0.6
A0B100GF1.0	27.7 ± 0.3	37.7 ± 1.0	38.3 ± 2.4	36.1	1.6	18.9 ± 2.1	3.0 ± 0.1	0.49	0.16	6.3 ± 0.2
A0B100GF1.5	29.1 ± 1.7	38.5 ± 2.5	40.7 ± 1.1	32.3	5.7	20.2 ± 3.9	3.2 ± 0.1	0.50	0.16	7.3 ± 0.2
A75B25GF1.0	30.7 ± 1.3	37.6 ± 0.2	40.7 ± 1.4	22.5	8.2	20.4 ± 1.5	2.9 ± 0.2	0.50	0.14	7.2 ± 0.4
A50B50GF1.0	31.3 ± 1.3	37.9 ± 1.0	41.2 ± 0.8	21.1	8.7	21.1 ± 2.3	3.0 ± 0.2	0.51	0.14	8.3 ± 0.5
A25B75GF1.0	32.4 ± 0.6	40.2 ± 0.7	42.2 ± 0.3	24.1	5.0	22.0 ± 0.9	3.5 ± 0.2	0.52	0.16	8.6 ± 0.5

[a] Increase in f_{cu} from 1 to 7 days. [b] Increase in f_{cu} from 7 to 28 days.

Incorporating different combinations of short and long GF had a limited impact on f_{cu}. For instance, increasing the replacement percentage of short with long fibers from 25% to 50% and from 50% to 75% increased 1-day f_{cu} by 2% and 6%, respectively. Meanwhile, 7- and 28-day f_{cu} increased by up to 7% and 4%, respectively. Furthermore, incorporating hybrid GF combinations in geopolymer concrete enhanced f_{cu} at all ages compared to their counterpart mixes in series A and B. In comparison with mix A100B0GF1.0 of series A, the 1-, 7-, and 28-day f_{cu} of hybrid mixes increased, on average, by 20%, 14%, and 10%, respectively. Conversely, compared to mix A0B100GF1.0 in series B, the respective strengths were, on average, 14%, 3%, and 8% higher. In addition, the f_{cu} of hybrid mixes was superior to counterparts reinforced with a single type of GF at a higher volume fraction of 1.5%. These results show that the compressive strength of slag-fly ash geopolymer concrete could be improved to a greater extent by utilizing a hybrid combination of GF rather than increasing the volume fraction when incorporating a single type of GF. This is due to the ability of short and long GF to bridge microcracks and prevent macrocrack propagation, respectively [60]. Similar findings have been reported in other work on steel fiber-reinforced geopolymer concrete [24].

The percent increase in f_{cu} from 1 to 7 days and from 7 to 28 days for each mix is also shown in Table 7. The percent increases from 1 to 7 days are significantly higher than those from 7 to 28 days. For instance, the plain control mix had respective increases of 37.5% and 4.4% from 1 to 7 days and from 7 to 28 days. The higher strength increase within the first 7 days is mainly owed to the coupled formation of calcium aluminosilicate (C-A-S-H) and calcium silicate hydrate (C-S-H) gels during the geopolymerization process [61–64]. However, the continuous strength development until 28 days is associated with the formation of sodium aluminosilicate hydrate (N-A-S-H) gel from the geopolymerization of fly ash [61,63].

Furthermore, mixes of series A and B mixes experienced different strength development profiles. For mixes incorporating type A (short) GF at 0.5%, 1.0%, and 1.5% volume fractions, by volume, the strength development decreased by 5%, 8%, and 8%, respectively, compared to the control mix, even though the strength values were higher due to fiber incorporation. Such reduction in strength development is owed to the higher 1-day strength in GF-reinforced geopolymer concrete mixes. Conversely, the strength development between 7 and 28 days increased by 5%, 6%, and 3% upon the inclusion of 0.5%, 1.0%, and 1.5% short GF volume fractions. For mixes made with type B GF or a hybrid combination of GF, the strength development from 1 to 7 days was generally lower than that of the control mix, except for mixes made with type B GF at volume fractions of 0.5 and 1.0%. Meanwhile, these two mixes had inferior strength gain from 7 to 28 days to the control mix, while other mixes were superior. It appears that the addition of type A short GF had a more prominent effect on the strength gain over the first 7 days.

The 28-day cylinder compressive strength, f'_c, for slag-fly ash blended geopolymer concrete mixes are presented in Table 7. Similar to the 28-day f_{cu}, increasing the volume fraction of either type (A or B) of GF increased the value f'_c. Incorporating 0.5%, 1.0%, and 1.5% of short GF in geopolymer concrete mixes resulted in 15%, 31%, and 42% respective increases in f'_c compared to the control mix. Conversely, incorporating long GF in mixes at

similar volume fractions resulted in 13%, 52%, and 62% respective increases in f'_c. Longer fibers were more effective at increasing f'_c than shorter counterparts. Such an increase in f'_c is owed to the improved bridging effect provided by longer GF. Similar findings have been reported in another work on concrete reinforced with steel fibers [23]. Moreover, combining the two types of GF, i.e., hybrid, led to higher f'_c values than those mixes reinforced with a single type of GF and the control mix. Further increases in long GF in a hybrid combination resulted in higher 28-day f'_c. Furthermore, it can be observed that a mix with 1.5% short or long GF volume fraction (A100B0GF1.5 or A0B100GF1.5) resulted in a lower f'_c than any of the hybrid mixes. This observation indicates that higher compressive strengths can be obtained in slag-fly ash blended geopolymer concrete by using a hybrid of two types of GF rather than increasing the volume fraction of a single type of GF.

The ratio of f'_c-to-f_{cu} is also presented in Table 7. The ratio of the control mix was 0.37, indicating a significant difference between the cylinder and cube compressive strengths. Similar low f'_c-to-f_{cu} ratios were also reported in previous studies for plain slag, slag-fly ash, and silica fume/slag-based geopolymer concretes [65–67]. It seems that geopolymer concrete is more sensitive to the slenderness effect than cement-based concrete. Such a fact should be considered by practitioners and researchers when designing based on the values of f_{cu}. The f'_c-to-f_{cu} ratio increased upon increasing the GF volume fraction. This indicates that the cylinder slenderness effect was reduced as more GF were added into the geopolymer concrete mix. The inclusion of short GF of 0.5%, 1.0%, and 1.5%, by volume, resulted in higher ratios of 0.39, 0.43, and 0.44, respectively, while the addition of longer GF at similar volume fractions resulted in 0.37, 0.49, and 0.50, respectively. Meanwhile, the inclusion of a hybrid combination of GF at a 1% volume fraction resulted in an average f'_c-to-f_{cu} ratio of 0.51. A correlation exists between the cylinder and cube compressive strengths. As shown in Figure 9, a linear relationship (Equation (7)) was developed using regression analysis to predict f'_c from f_{cu} and vice versa with good accuracy (R^2 = 0.88). However, this relationship is limited to f_{cu} values exceeding 23.6 MPa and to the mixes examined in this study.

$$f'_c = 1.16 f_{cu} - 27.41 \quad (7)$$

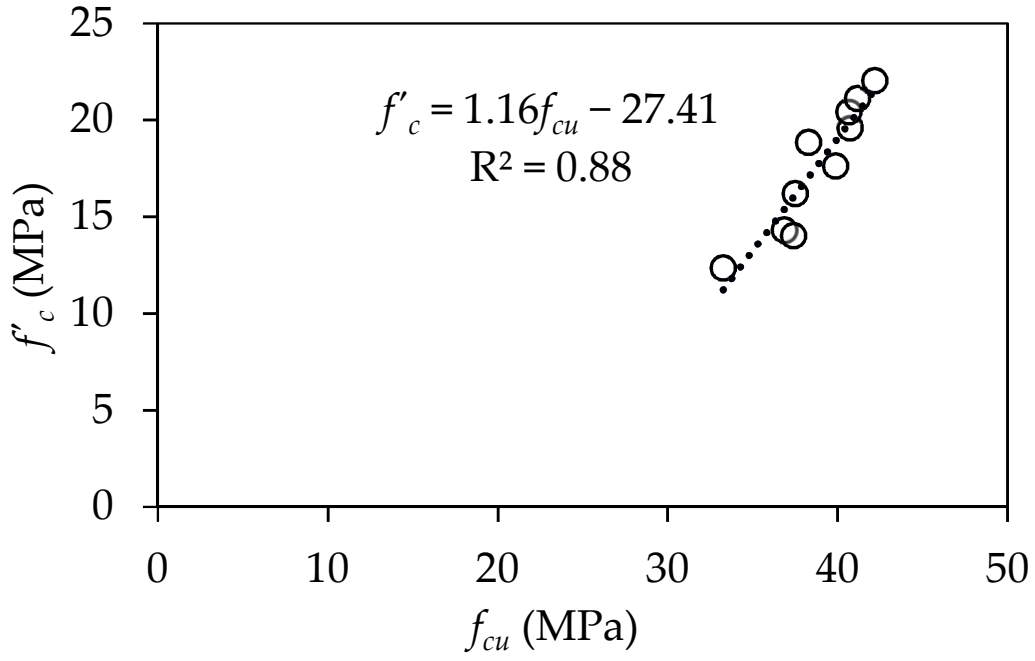

Figure 9. Relationship between the cylinder and cube compressive strengths at 28 days.

3.6. Compressive Stress–Strain Response

The axial compressive stress–strain curves of 28-day cylinder concrete specimens are illustrated in Figure 10. The peak stresses of mixes with GF were higher than those of the plain control mix. The peak stress increased by 30%, 61%, and 110% upon the inclusion of short GF at 0.5%, 1.0%, and 1.5% volume fractions, respectively. Conversely, incorporating long GF at similar respective volume fractions resulted in 43%, 96%, and 114% higher peak stress compared to the control mix. As such, it can be estimated that every 0.5% addition of short and long GF enhanced the peak stress by, on average, 36% and 38%, respectively. This indicates that the inclusion of long GF is slightly more impactful than short GF on the peak stress. Mixes including long GF at 0.5%, 1.0%, and 1.5% volume fractions resulted in 13%, 35%, and 4% higher stresses, respectively, than those incorporating short counterparts.

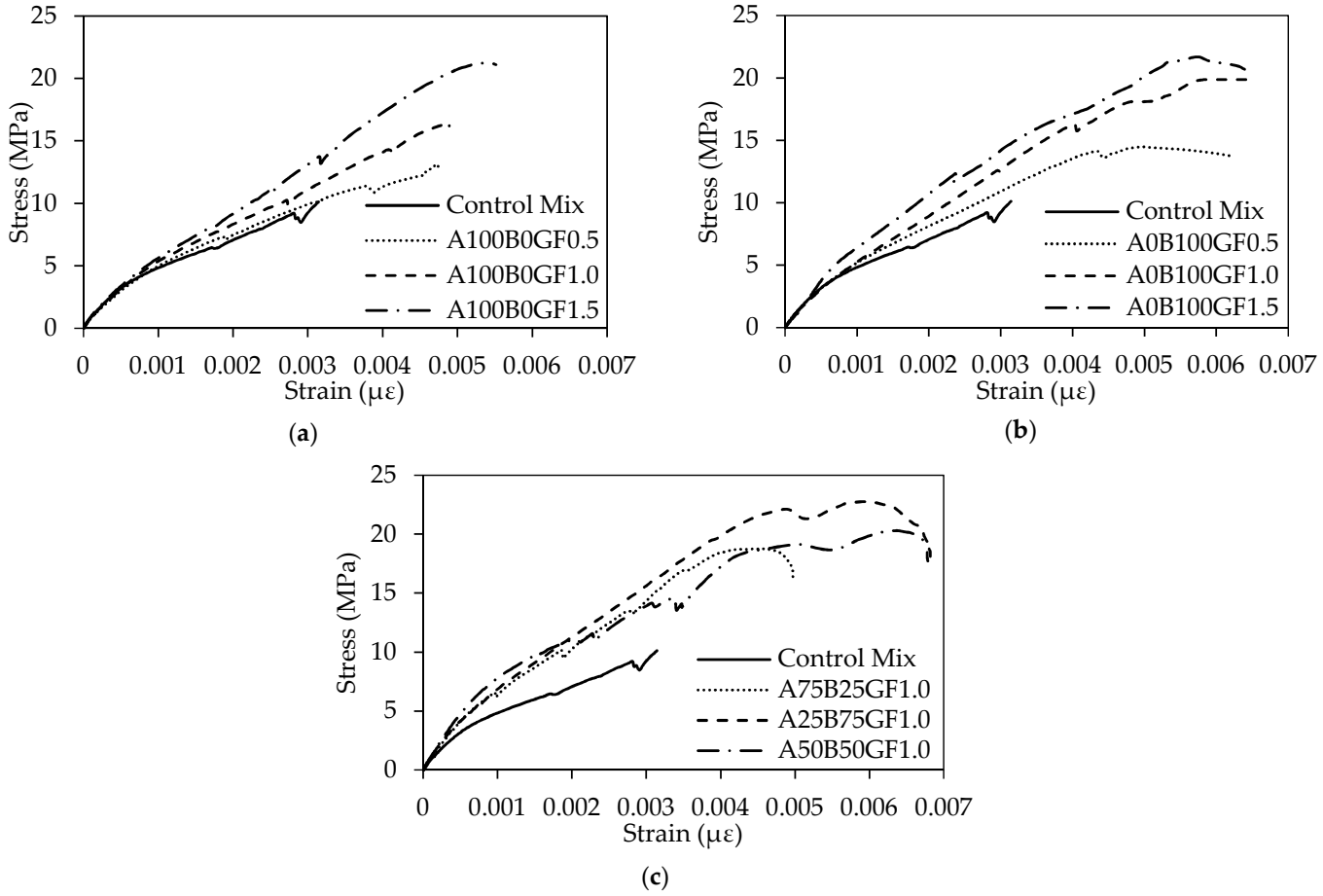

Figure 10. Typical compression stress–strain curves of cylinder concrete specimens for (**a**) Series A, (**b**) Series B, and (**c**) Series C.

The stress–strain response of mixes with different hybrid GF combinations, i.e., series C, is presented in Figure 10c. Mixes incorporating hybrid GF combinations had higher peak stresses than those with one type of GF and the control mix. The peak stress increased by 86%, 101%, and 125% upon combining short and long GF at A-to-B of 3:1, 1:1, and 1:3, respectively, in comparison to the control mix. Furthermore, compared to the counterpart non-hybrid mix in series A with a similar volume fraction (1.0%), replacing 25%, 50%, and 75% of short with long GF resulted in a 15%, 24%, and 40% increase in the peak stress. Furthermore, mixes incorporating more than 50% of long GF resulted in superior results to that made with a single type, i.e., 100%. As such, incorporating a hybrid combination with a 75% replacement percentage of short with long GF, i.e., A:B of 1:3, at a volume fraction of 1.0%, had superior peak stress.

The addition of GF to slag-fly ash blended geopolymer concrete increased the maximum strain. Compared to the control mix, the inclusion of 0.5%, 1.0%, and 1.5% short GF increased the strain by 51%, 56%, and 76%, respectively, while the addition of long GF at similar volume fractions increased the maximum strains by 97%, 104%, and 103%, respectively. While both types of GF improved the deformability of geopolymer concrete, the effect of longer GF was more prominent. Furthermore, mixes with hybrid GF combinations enhanced the deformability, with those having A-to-B ratios of 1:1 and 1:3 being superior. Evidently, the addition of GF enhanced the compressive behavior and deformability of slag-fly ash blended geopolymer concrete, owing to the bridging effect of the GF. Similar outcomes were noted in cement and geopolymer concrete made with steel fibers [68–70].

3.7. Modulus of Elasticity

The modulus of elasticity results, E_c, of slag-fly ash blended geopolymer concrete mixes with types A and/or B of GF are presented in Table 7. The addition of 0.5%, 1.0%, and 1.5% short glass fiber volume fractions, by volume, increased the E_c by 17%, 26%, and 47%, respectively, compared to the plain control mix. Conversely, the addition of long GF at similar volume fractions led to 21%, 37%, and 59% respective increases in E_c. Thus, it is clear that long GF were more influential on E_c than short counterparts. Moreover, replacing 25%, 50%, and 75% of short GF with long ones in hybrid mixes resulted in 56%, 80%, and 87% increases in E_c, respectively, in comparison to the control mix. Such enhancement is owed to the increase in compressive strength and stress, S_2, in Equation (1), and restriction in crack formation and propagation, as concluded in other work on steel fiber-reinforced geopolymer concrete [65,66]. Experimental results indicate that increasing the GF volume fraction enhanced E_c, with long GF being more effective than short ones. In addition, further enhancement was noted in hybrid GF mixes at a 1% volume fraction, where the geopolymer mix made with GF at A-to-B of 1:3 presented superior performance. Steel fiber-reinforced geopolymer concrete experienced similar increases in E_c with longer fibers and hybrid combinations of steel fibers [25].

Results of E_c are synonymous with those of f'_c. As such, a relationship was established between the two properties. Figure 11a illustrates a relationship between E_c and f'_c. Equation (8) presents a tool to predict E_c from f'_c with a correlation coefficient, $R^2 = 0.91$. However, the proposed model is limited to values of f'_c exceeding 4.1 MPa.

$$E_c = 3.05\sqrt{f'_c} - 6.18 \quad (8)$$

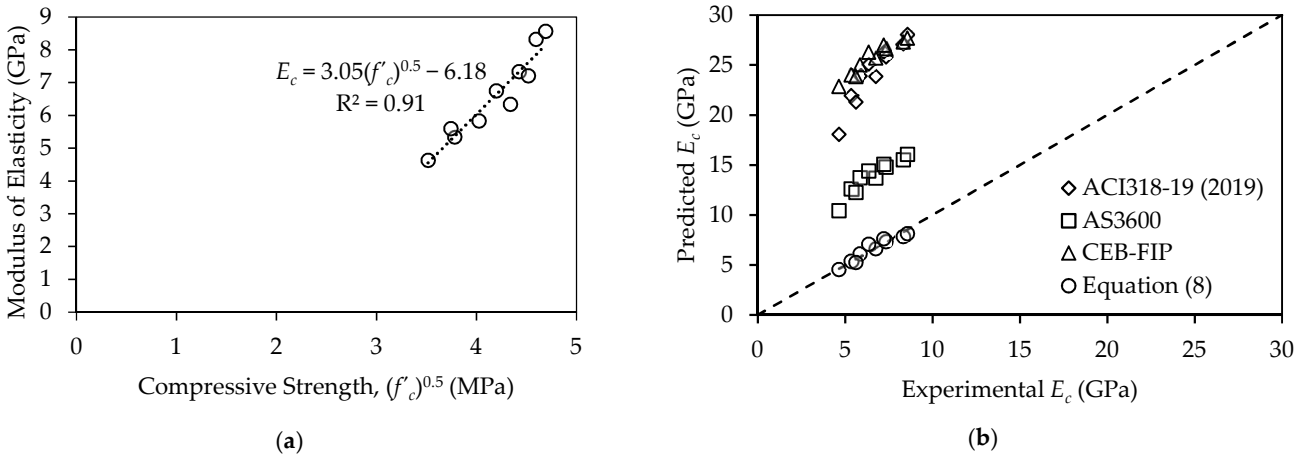

(**a**) (**b**)

Figure 11. (**a**) Relationship between E_c and f'_c at the age of 28-days. (**b**) Experimental versus predicted modulus of elasticity, E_c.

The obtained relationship in Equation (8) was compared to those developed by ACI 318-19 [71], CEB-FIP [72], and AS3600 [73] (Table 8), as illustrated in Figure 11b. With scatter points converging on the 45° line, the model developed in Equation (8) provides a relatively more accurate prediction of E_c than the codified equations. It can be observed that the codified models developed by ACI 318-19 [71], CEB-FIP [72], and AS3600 [73] overestimated the E_c of the mixes presented in this work. These equations were developed for conventional cement-based concrete without fiber reinforcement. As such, their applicability to glass fiber-reinforced slag-fly ash blended geopolymer concrete may be limited. Nevertheless, the AS3600 [73] model followed a similar trend as Equation (8) and could thus be used to predict the values of E_c produced herein subject to modifying it with a factor of 0.512.

Table 8. Equations relating the modulus of elasticity to the cylinder compressive strength.

Reference	Modulus of Elasticity (E_c)
ACI 318-19 [71]	$0.043\ w^{1.5}\ {f'_c}^{0.5}$
CEB-FIP [72]	$9979.4\ {f'_c}^{0.33}$
AS3600 [73]	$0.024\ w^{1.5}\ ({f'_c}^{0.5} + 0.12)$

w = density of concrete at 28 days (kg/m^3). f'_c = compressive strength (MPa).

3.8. Splitting Tensile Strength

The splitting tensile strength (f_{sp}) was used to indirectly evaluate the tensile performance of 28-day glass fiber-reinforced slag-fly ash blended geopolymer concrete. Table 7 presents f_{sp} for all mixes. A similar trend was noted as that of f'_c, where increasing the GF volume fraction increased f_{sp}. Incorporating short GF at 0.5%, 1.0%, and 1.5%, by volume, enhanced f_{sp} by 15%, 21%, and 30% compared to the plain control mix. Further enhancement in f_{sp} was noted when utilizing long GF at similar volume fractions, with respective increases of 16%, 36%, and 41% compared to the control mix. This signifies that long GF were more effective at improving f_{sp} than their short counterparts. Moreover, the inclusion of hybrid GF at 1%, by volume, with A-to-B ratios of 3:1, 1:1, and 1:3 led to 29%, 33%, and 58% higher f_{sp}, respectively, with reference to the control mix. Evidently, hybridization is more efficient than single fiber incorporation to enhance the f_{sp} of slag-fly ash blended geopolymer concrete. Similar findings were found in a study conducted by Park et al. [74], in which utilizing a combination of macro and micro steel fibers in ultrahigh-performance concrete provided superior performance to a counterpart reinforced with a single type of steel fiber. Nevertheless, GF addition was more impactful on E_c than on f_{sp}, unlike what has been reported in steel fiber-reinforced geopolymers [25].

Table 7 also presents the ratio of f_{sp}-to-f'_c. It varied between 0.14 and 0.19, which is slightly higher than the ratio reported in steel fiber-reinforced geopolymer concrete [24,25]. A reduction in the ratio was observed upon the addition of GF. This implies that GF were slightly more influential on f'_c rather than f_{sp}. Nevertheless, the ratio was more influenced by increasing the volume fraction of GF. Mixes with hybrid GF resulted in the lowest f_{sp}-to-f'_c ratios. Despite an increase in f_{sp} up to 58%, the increase in f'_c reached 77%, resulting in lower ratios. Nevertheless, the effect of GF inclusion on f_{sp} and f'_c is similar. Accordingly, Equation (9) was developed to correlate the two properties, as shown in Figure 12a. With a correlation coefficient R^2 of 0.96, it is possible to predict f_{sp} from f'_c with high accuracy.

Furthermore, Equation (9) was compared to the codified equations presented in Table 9 that are used to predict f_{sp} from f'_c. Figure 12b illustrates the experimental and predicted f_{sp} results. The models developed by ACI 318-19 [71], CEB-FIB [72], and AS3600 [73] relatively underestimated the f_{sp} of geopolymer mixes produced in this work, while that of Equation (9) was more reliable here, as it converged on the 45°-line. The ACI 318-19, AS3600, and CEB-FIP models resulted in, on average, 80%, 53%, and 72% lower values, respectively. Hence, by introducing correction factors, shown in Table 9, the codified equations could be adjusted to be suitable for glass fiber-reinforced slag-fly ash blended geopolymer concrete

presented herein. Still, the codified equations were developed for plain cement-based concrete and are used herein for comparison purposes.

$$f_{sp} = 0.68\sqrt{f'_c} \quad (9)$$

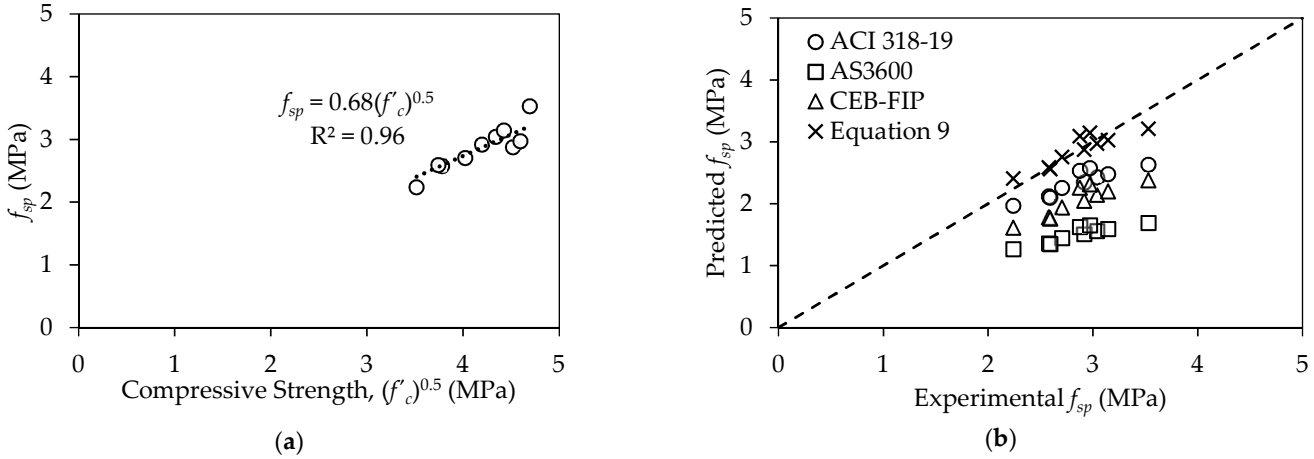

Figure 12. (**a**) Correlation between splitting tensile strengths, f_{sp}, and compressive strength, f'_c. (**b**) Experimental versus predicted splitting tensile strengths, f_{sp}.

Table 9. Equations relating splitting tensile strength and compressive strength.

Reference	Tensile Strength (f_{sp})	Correction Factor	Modified Equations
ACI 318 [71]	$0.56f'_c{}^{0.5}$	1.21	$0.68f'_c{}^{0.5}$
CEB-FIP [72]	$0.30f'_c{}^{0.67}$	1.28	$0.38f'_c{}^{0.67}$
AS3600 [73]	$0.36f'_c{}^{0.5}$	1.88	$0.68f'_c{}^{0.5}$

3.9. Water Absorption

The infiltration of moisture and other aggressive liquids into the interconnected pores of concrete causes a deterioration in its quality. Since water is the primary carrier of aggressive ions into the concrete, its durability can be directly evaluated by its ability to absorb water [75]. The results of water absorption at 28 days are presented in Table 10. The inclusion of GF caused a decrease in water absorption. The largest water absorption of 6.5% was seen in the control specimen (A0B0GF0.0). The mixes with short GF of series A at 0.5%, 1.0%, and 1.5% had corresponding water absorption rates of 5.5%, 5.4%, and 4.4%, respectively. In contrast to series B mixes, at similar volume fractions, the respective water absorption rates were 5.4%, 4.9%, and 4.3%. In accordance with the abovementioned data and in comparison to the control mix, the addition of 0.5%, 1.0%, and 1.5% GF volume fractions caused a decrease in the water absorption by 15%, 17%, and 32% for short GF and 17%, 24%, and 34% for long GF, respectively. Furthermore, water absorption of 4.3%, 4.0%, and 3.8% was noted in mixes with 25%, 50%, and 75% replacement percentages of short GF with long ones, respectively. In reference to the control mix, the respective decreases were 34%, 38%, and 42%. Such reduction in water absorption, caused by GF inclusion, is associated with an improvement in the mechanical properties and an increase in the hardened density. Similar findings have been reported by Saral et al. [55] in fly ash based geopolymer concrete reinforced with GF.

Table 10. Water absorption and sorptivity of geopolymer concrete mixes.

Mix Designation	Water Absorption (%)	Sorptivity (mm/s$^{0.5}$)
A0B0GF0.0	6.46 ± 0.33	0.037 ± 0.002
A100B0GF0.5	5.47 ± 0.22	0.044 ± 0.002
A100B0GF1.0	5.37 ± 0.33	0.045 ± 0.003
A100B0GF1.5	4.38 ± 0.25	0.044 ± 0.003
A0B100GF0.5	5.38 ± 0.38	0.048 ± 0.004
A0B100GF1.0	4.91 ± 0.20	0.051 ± 0.003
A0B100GF1.5	4.28 ± 0.26	0.062 ± 0.004
A75B25GF1.0	4.28 ± 0.22	0.060 ± 0.003
A50B50GF1.0	4.02 ± 0.29	0.057 ± 0.004
A25B75GF1.0	3.75 ± 0.30	0.062 ± 0.005

3.10. Sorptivity

The sorptivity test is used to evaluate the tendency of concrete to absorb and transport water through capillary action into its microstructure. The strength of capillary forces, permeability, porosity, structure, and distribution of pores in concrete mainly affect the sorptivity, i.e., rate of absorption [25].

Figure 13 presents a scatter plot of the water absorption against the square root of time. During the first 60 min, the slope of the sorptivity curve was higher than that of the remaining test duration. This was a result of the consecutive filling of larger and small voids at the early stages. The curves of capillary sorptivity of concrete mixes with short (type A) GF are illustrated in Figure 13a. An increase in water absorption rates was seen in series A mixes. In comparison to the control mix, the addition of short GF by 0.5%, 1.0%, and 1.5% by volume increased the absorption rates by 18%, 20%, and 17%. In addition, the results of series B mixes are illustrated in Figure 13b. Contrary to the control mix, the addition of long GF at 0.5%, 1.0%, and 1.5% volume fractions, by volume, resulted in an increase in water absorption rates by 29%, 36%, and 67%, respectively.

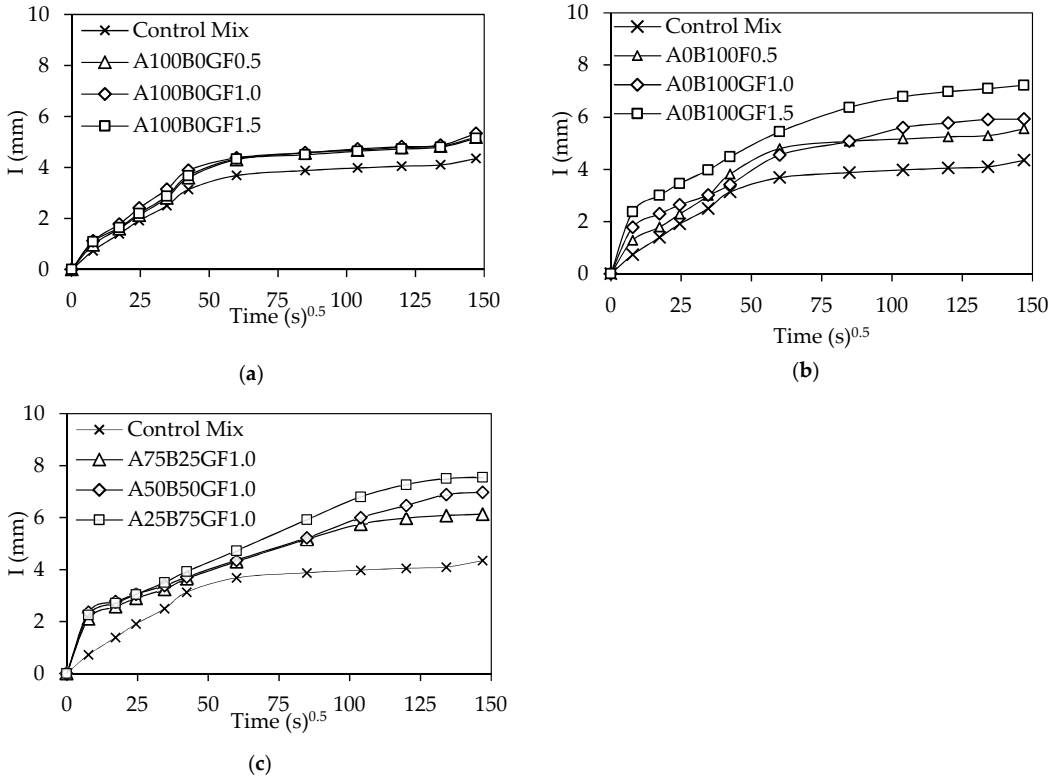

Figure 13. Absorption of geopolymer concrete mixes over time: (**a**) Series A, (**b**) Series B, and (**c**) Series C.

For series C hybrid mixes, the absorption rates versus the square root of time are depicted in Figure 13c. The initial slope was higher in hybrid mixes. It was seen that an increase in sorptivity by 60%, 52%, and 67%, resulted from replacing 25%, 50%, and 75% of short (type A) with long (type B) GF, respectively, compared to the control mix. A similar initial rate of absorption was seen in the geopolymer concrete mixture with 75% replacement of short with long fibers (A25B75GF1.0) and a non-hybrid mixture consisting of only long GF at 1.5% volume fraction (A0B100GF1.5).

Typically, the addition of fibers to concrete causes a restriction in water movement and the filling of void space in the concrete structure [76]. In this work, the inclusion of GF led to a decrease in the water absorption of slag-fly ash blended geopolymer concrete; however, the rate of absorption, i.e., sorptivity, increased. Despite having lesser voids than plain counterparts, it is believed that the addition of GF resulted in the interconnectivity of the voids. A similar phenomenon was reported by Kwan et al. [77], where the addition of GF led to the formation of additional interfacial bonds and voids, which provided a route for water passage through the concrete. Nevertheless, despite the increase in the connectivity of the voids, i.e., higher sorptivity, due to the addition of GF, the total void content, represented by the water absorption, decreased. In conjunction with the ultrasonic pulse velocity (UPV) results presented later, it can be concluded that the incorporation of GF in slag-fly ash blended geopolymer concrete enhanced its mechanical and durability properties.

3.11. Abrasion Resistance

The capacity of concrete to resist wear caused by impact and friction defined the abrasion resistance of concrete. After exposing the samples to 500 revolutions in an LA abrasion machine, the resulting mass loss is a measurement of the abrasion resistance of concrete. The mass loss profile of slag-fly ash blended geopolymer concrete with different GF volume fractions and proportions is presented in Figure 14. A total mass loss, i.e., 100% mass loss, at 200 revolutions was noted in the control mix, while such a total mass loss was extended to at least 400 revolutions by the incorporation of either type of GF. Abrasion mass losses (at 500 revolutions) of 100% were seen in series A mixes incorporating up to 1.5% glass fiber volume fractions, as shown in Figure 14a. The mass loss for mixes made with 0.5%, 1.0%, and 1.5% was 100%, 93%, and 93% at 400 revolutions. Conversely, reductions in the abrasion mass loss by 4%, 11%, and 32% were observed as a result of incorporating 0.5%, 1.0%, and 1.5% long GF volume fractions, respectively, at 400 revolutions (Figure 14b). Nevertheless, the rate of mass loss diminished as the GF volume fraction (for both types of fibers) increased. Similar findings have been reported in past work on the use of fibers in conventional and geopolymer concrete [59,64].

Figure 14c illustrates mixes with hybrid combinations of GF. In comparison with the control mix, substituting 25%, 50%, and 75% of short GF with long ones resulted in 14%, 36%, and 38% reductions in the mass loss at 500 revolutions. Consequently, an improvement in the abrasion resistance (i.e., lower mass loss) can be achieved by increasing the long GF content in hybrid mixes. Slag-fly ash blended geopolymer concrete reinforced with a hybrid combination of GF was more resistant to abrasion than those made with a single type of GF even when a higher volume fraction was used in the mix.

The abrasion mass loss results are inversely proportional to the 28-day cylinder compressive strength (f'_c). Thus, it is possible to develop a relationship between these two properties for mixes having an abrasion mass loss of less than 100%. Figure 15 illustrates the developed linear relationship. It is also expressed in Equation (10), where AR represents the abrasion mass loss in percent. Evidently, it is possible to predict the abrasion resistance from f'_c of blended geopolymer concrete made with different types, volume fractions, and combinations of GF with good accuracy (R^2 = 0.91). The proposed equation is only applicable to mixes that resulted in less than 100% abrasion mass loss and those with f'_c more than 19 MPa.

$$AR(\%) = -13.34\left(f'_c\right) + 354.27 \quad (10)$$

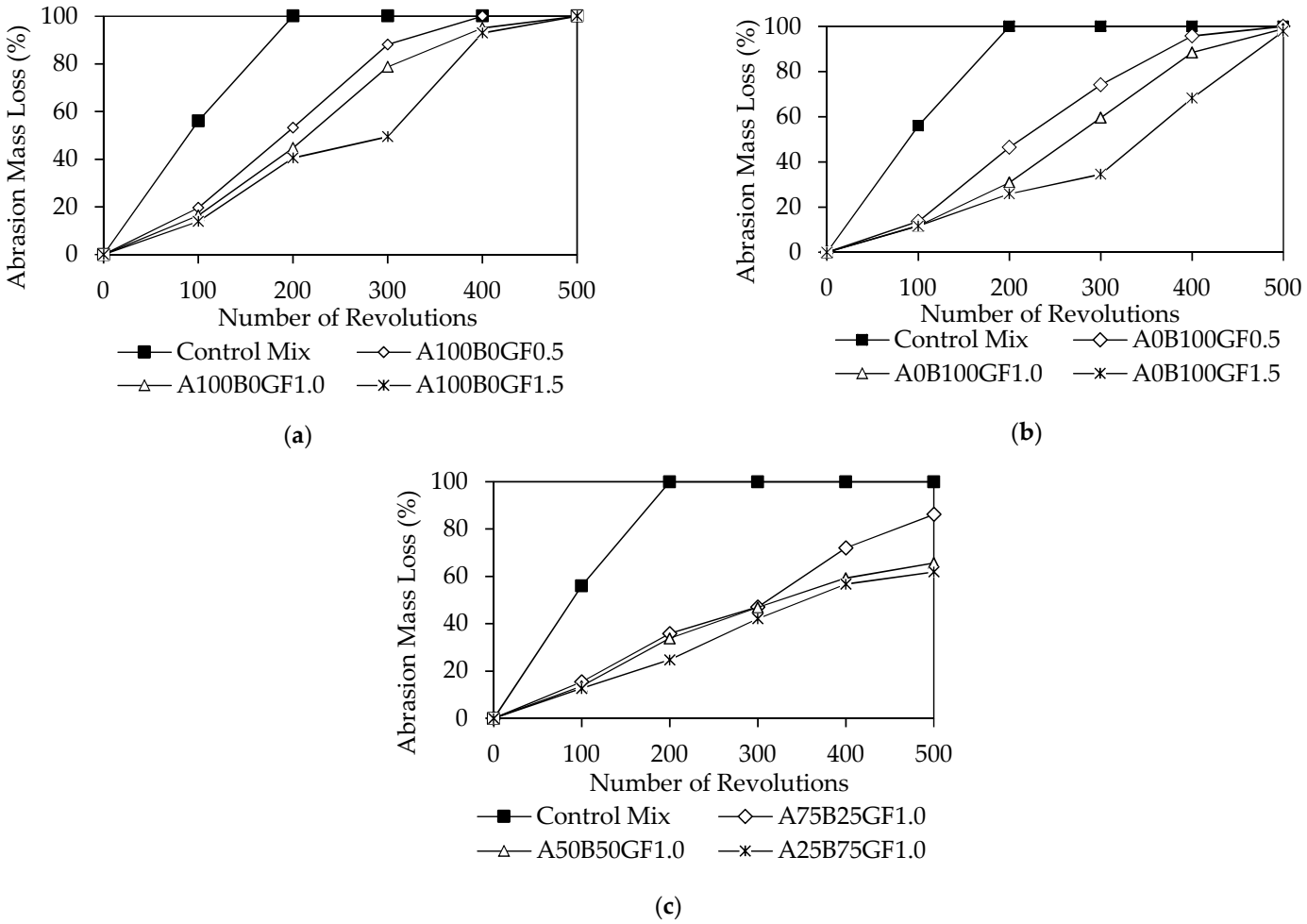

Figure 14. Abrasion resistance of: (**a**) Series A, (**b**) Series B, and (**c**) Series C mixes.

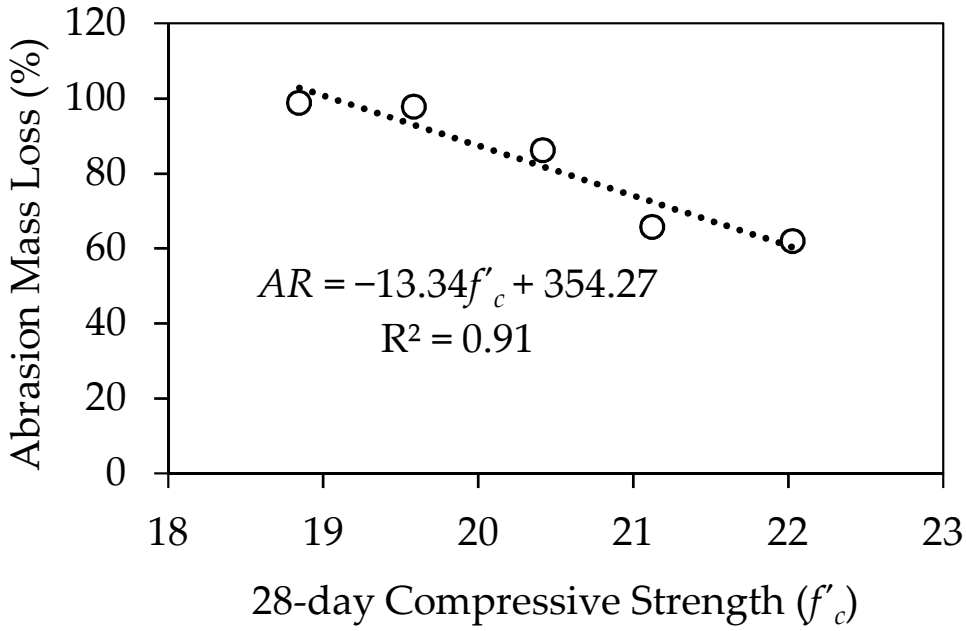

Figure 15. Relationship between abrasion resistance and 28-day compressive strength.

3.12. Ultrasonic Pulse Velocity

Assessing the concrete strength and general quality can be achieved by utilizing the UPV test. The UPV test results, expressed as velocity (m/s), for slag-fly ash blended geopolymer concrete mixes at 28 days are presented in Figure 16. The lowest and highest velocities were for the control and A25B75GF1.0 mixes, with respective values of 1031 and 3916 m/s. Such a low UPV (i.e., 1031 m/s) is owed to the relatively low f'_c and high absorption values, as was reported in fly ash based geopolymer concrete [78]. Concrete specimens were considered as "excellent", "good", "average", and "poor" for UPV values falling in the respective ranges of above 4500, 3500–4500, 3000–3500, and below 3000 m/s according to BS 1881 [79]. While the control plain mix fell within the "poor" range, the addition of hybrid and single GF at different volume fractions resulted in higher UPV values, i.e., produced a better quality concrete that fell within the "average" and "good" ranges. Velocities of 3076, 3247, and 3281 m/s were achieved in series A mixes with 0.5, 1.0, and 1.5% short GF volume fractions, respectively. Similar volume fractions in series B mixes achieved velocities of 3254, 3719, and 3894 m/s, respectively. Only two out of all non-hybrid mixes fell within the "good" concrete quality range (A0B100GF1.0 and A0B100GF1.5), while the remaining mixes were classified as having "average" concrete quality. The hybrid mixes of series C were considered to be of "good" quality, as their velocities were 3747, 3763, and 3916 m/s. Such enhancement in UPV values is a direct indication of the decrease in void content (i.e., water absorption) in samples with glass fibers, correspondingly resulting in better mechanical and durability properties. A similar phenomenon was noted in cement-based concrete upon the addition of steel fibers [59].

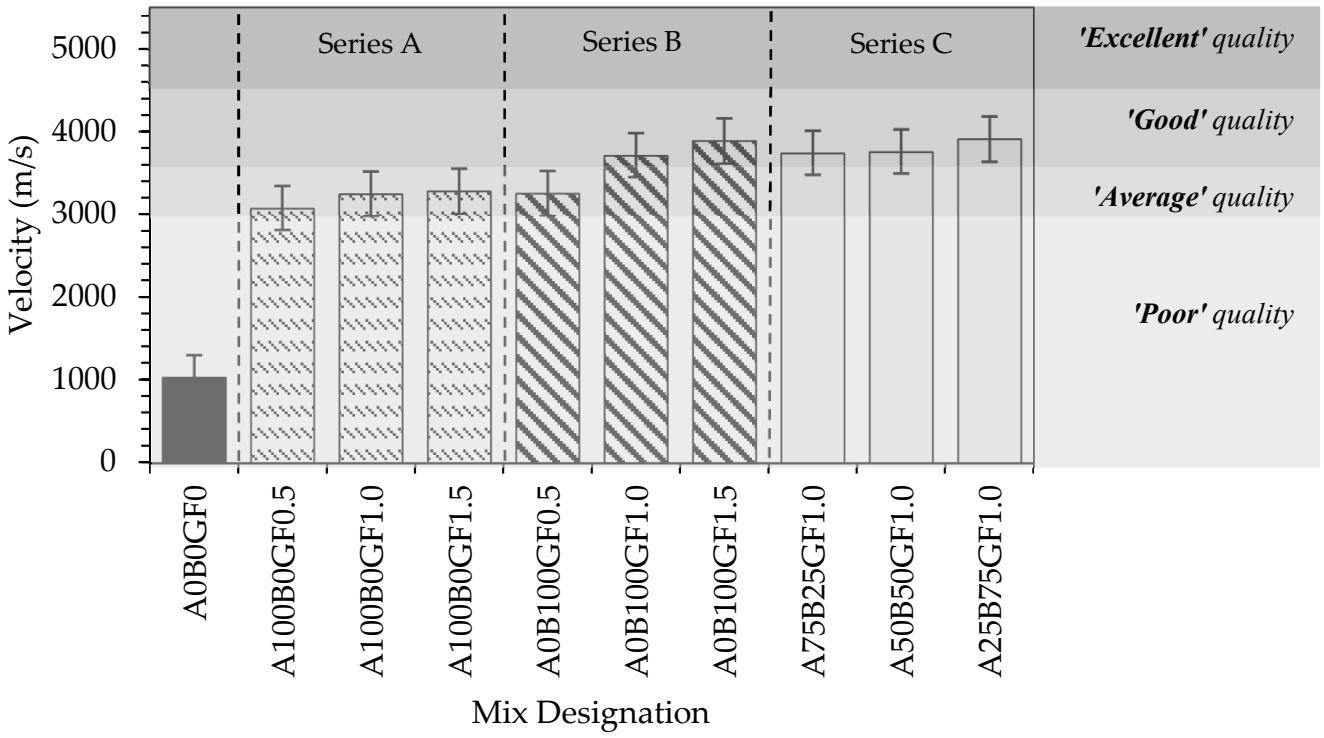

Figure 16. UPV of glass fiber reinforced geopolymer concrete.

4. Conclusions

The fresh and hardened properties of glass fiber-reinforced slag-fly ash blended geopolymer concrete mixes were evaluated. The effects of different types, volume fractions, and combinations of glass fibers (GF) were examined. Based on the experimental test results, the following conclusions can be drawn:

- The slump decreased by up to 75% as GF were added to the geopolymer concrete mix with a more drastic effect being noted with the addition of long GF. The incorporation

of a hybrid GF combination at a 1% volume fraction led to better workability results, as it reduced the effect of fiber interlocking.

- Increasing the GF volume fraction and length led to up to 18% lower compaction factors and 43% higher vebe times than that of the plain concrete mix. Mixes with hybrid glass fiber combinations were better than those with a single type of GF.
- The addition of different types, volume fractions, and combinations of GF enhanced 1, 7, and 28-day compressive strengths of geopolymer concrete. Increasing the GF volume fraction resulted in a decrease in compressive strength development between 1 and 7 days with respect to the plain control mix. Mixes with a 1.5% long GF volume fraction resulted in the highest strength development at later ages. Hybrid GF-reinforced mixes exhibited larger strength development at an early age; however, increasing the amount of long GF in a hybrid combination delayed strength development.
- An increase of up to 24% in compressive strength was noted upon incorporating short GF in geopolymer concrete. The addition of long GF decreased the compressive strength up to 7 days but then increased it at 28 days. A significant increase of up to 40% in compressive strength was noted when incorporating hybrid GF combinations with more long GF at a 1% volume fraction.
- The addition of glass fibers enhanced the peak stress and strain upon increasing the length and volume fraction of GF. Mixes with hybrid glass fiber combination at a ratio (A:B) of 1:1 and 1:3 at 1% volume fraction exhibited similar stress and strain of that mixed with long GF at 1.5%. The modulus of elasticity (E_c) was improved by up to 46% and 59% upon incorporating short and long GF, respectively. A further enhancement of 85% was noted when hybridizing GF.
- The 28-day splitting tensile (f_{sp}) strength increased by up to 30% and 41% with the inclusion of short and long GF, respectively. However, a hybrid mix with a proportion ratio (A:B) of 1:3 had a superior tensile strength of 3.5 MPa.
- The water absorption decreased by up to 34% with the addition of glass fibers with respect to the control mix. Incorporating a hybrid GF combination further decreased the water absorption by up to 42%. Contrarily, the initial sorptivity increased upon the addition of glass fibers, up to 67%. This is owed to the higher connectivity of voids and larger interfacial voids caused by glass fibers.
- The abrasion resistance of geopolymer concrete mixes was improved upon the inclusion of GF, more so for long GF than for short counterparts. Further enhancement was found in mixes with hybrid GF combinations at a 1% volume fraction.
- Results of 28-day f_{cu} were correlated to that of 28-day f'_c. Correlation equations were also developed relating each of f_{sp}, E_c, and abrasion resistance to 28-day f'_c. Codified equations developed for plain cement-based concrete provided fewer representative results. The difference in concrete chemistry and the addition of fibers rendered these equations less accurate in predicting the properties of glass fiber-reinforced slag-fly ash geopolymer concrete.
- The use of GF enhanced the general quality of geopolymer concrete with up to 280% higher velocity values, according to the ultrasonic pulse velocity (UPV) test. While mixes reinforced with long GF and a high volume percentage (> 1%) or hybrid GF were classified as "good" quality, remaining mixes were categorized as "average."

Based on the experimental results and findings, it can be concluded that slag-fly ash blended geopolymer concrete reinforced with a hybrid glass fiber combination at a short fiber-to-long fiber ratio of 1:3 provided superior mechanical and durability properties. Future research is still needed to investigate the microstructure characteristics and flexural and shear performance of glass fiber-reinforced slag-fly ash blended geopolymer concrete.

Author Contributions: Conceptualization, H.E.-H., T.E.-M., and B.E.-A.; methodology, M.Z. and H.E.-H.; experimental work, M.Z.; validation, H.E.-H., T.E.-M., and B.E.-A.; investigation, M.Z. and H.E.-H.; resources, M.Z. and H.E.-H.; writing—original draft preparation, M.Z.; writing—review and editing, H.E.-H., T.E.-M., and B.E.-A.; visualization, H.E.-H., T.E.-M., and B.E.-A.; supervision, H.E.-H., T.E.-M., and B.E.-A.; project administration, H.E.-H.; funding acquisition, H.E.-H., T.E.-M., and B.E.-A. All authors have read and agreed to the published version of the manuscript.

Funding: This research was funded by the United Arab Emirates University, grant number 31N453.

Institutional Review Board Statement: Not applicable.

Informed Consent Statement: Not applicable.

Data Availability Statement: The data presented in this study are available on request from the corresponding author.

Conflicts of Interest: The authors declare no conflict of interest.

References

1. Cement: Production Ranking Top Countries 2020. Statista. Available online: https://www.statista.com/statistics/267364/world-cement-production-by-country/ (accessed on 17 February 2022).
2. Ma, C.-K.; Awang, A.Z.; Omar, W. Structural and material performance of geopolymer concrete: A review. *Constr. Build. Mater.* **2018**, *186*, 90–102. [CrossRef]
3. Benhelal, E.; Zahedi, G.; Shamsaei, E.; Bahadori, A. Global strategies and potentials to curb CO_2 emissions in cement industry. *J. Clean. Prod.* **2013**, *51*, 142–161. [CrossRef]
4. Herzog, H.; Eliasson, B.; Kaarstad, O. Capturing Greenhouse Gases. *Sci. Am.* **2000**, *282*, 72–79. [CrossRef] [PubMed]
5. Shaftel, H.; Callery, S.; Jackson, R.; Bailey, D. Overview: Weather, Global Warming and Climate Change. Climate Change: Vital Signs of the Planet. 2022. Available online: https://climate.nasa.gov/resources/global-warming-vs-climate-change (accessed on 12 February 2022).
6. Smith, A.B. *U.S. Billion-Dollar Weather and Climate Disasters, 1980–Present (NCEI Accession 0209268)*; NOAA National Centers for Environmental Information: Asheville, NC, USA, 2020. [CrossRef]
7. Raza, A.; El Ouni, M.H.; Azab, M.; Ali, K.; Haider, H.; Rashedi, A. A scientometric review on mechanical and durability performance of geopolymer Paste: Effect of various raw materials. *Constr. Build. Mater.* **2022**, *34*, 128297. [CrossRef]
8. El-Mir, A.; El-Hassan, H.; El-Dieb, A.; Alsallamin, A. Development and Optimization of Geopolymers Made with Desert Dune Sand and Blast Furnace Slag. *Sustainability* **2022**, *14*, 7845. [CrossRef]
9. Najm, O.; El-Hassan, H.; El-Dieb, A. Optimization of alkali-activated ladle slag composites mix design using taguchi-based TOPSIS method. *Constr. Build. Mater.* **2022**, *327*, 126946. [CrossRef]
10. El-Hassan, H.; Shehab, E.; Al-Sallamin, A. Effect of curing regime on the performance and microstructure characteristics of alkali-activated slag-fly ash blended concrete. *J. Sustain. Cem. Mater.* **2021**, *10*, 289–317. [CrossRef]
11. El-Hassan, H.; Shehab, E.; Al-Sallamin, A. Influence of Different Curing Regimes on the Performance and Microstructure of Alkali-Activated Slag Concrete. *J. Mater. Civ. Eng.* **2018**, *30*, 04018230. [CrossRef]
12. Baldovino, J.J.; Izzo, R.L.; Rose, J.L.; Domingos, M.D. Strength, durability, and microstructure of geopolymers based on recycled-glass powder waste and dolomitic lime for soil stabilization. *Constr. Build. Mater.* **2021**, *271*, 121874. [CrossRef]
13. Consoli, N.C.; Silvano, L.W.; Lotero, A.; Filho, H.C.S.; Moncaleano, C.J.; Cristelo, N. Key parameters establishing alkali activation effects on stabilized rammed earth. *Constr. Build. Mater.* **2022**, *345*, 128299. [CrossRef]
14. Davidovits, J. High-Alkali Cements for 21st Century Concretes. *ACI Symp. Publ.* **1994**, *144*, 383–398. [CrossRef]
15. Aleem, M.I.A.; Arumairaj, P.D. Geopolymer Concrete—A review. *Int. J. Eng. Sci. Emerg. Technol.* **2012**, *1*, 118–122. [CrossRef]
16. Allah, N.K.; El-Maaddawy, T.; El-Hassan, H. Geopolymer- and Cement-Based Fabric-Reinforced Matrix Composites for Shear Strengthening of Concrete Deep Beams: Laboratory Testing and Numerical Modeling. *Buildings* **2022**, *12*, 448. [CrossRef]
17. Abu Obaida, F.; El-Maaddawy, T.; El-Hassan, H. Bond Behavior of Carbon Fabric-Reinforced Matrix Composites: Geopolymeric Matrix versus Cementitious Mortar. *Buildings* **2021**, *11*, 207. [CrossRef]
18. Thomas, R.J.; Lezama, D.; Peethamparan, S. On drying shrinkage in alkali-activated concrete: Improving dimensional stability by aging or heat-curing. *Cem. Concr. Res.* **2017**, *91*, 13–23. [CrossRef]
19. El Ouni, M.H.; Raza, A.; Haider, H.; Arshad, M.; Ali, B. Enhancement of mechanical and toughness properties of carbon fiber-reinforced geopolymer pastes comprising nano calcium oxide. *J. Aust. Ceram. Soc.* **2022**, 1–13. [CrossRef]
20. Raza, A.; Khan, Q.U.Z.; El Ouni, M.H.; Brahmia, A.; Berradia, M. Mechanical Performance of Geopolymer Composites Containing Nano-Silica and Micro-Carbon Fibers. *Arab. J. Sci. Eng.* **2022**. [CrossRef]
21. Rashedi, A.; Marzouki, R.; Raza, A.; Rawi, N.F.M.; Naveen, J. Mechanical, Fracture, and Microstructural Assessment of Carbon-Fiber-Reinforced Geopolymer Composites Containing Na_2O. *Polymers* **2021**, *13*, 3852. [CrossRef]

22. Ali, L.; El Ouni, M.H.; Raza, A.; Janjua, S.; Ahmad, Z.; Ali, B.; Ben Kahla, N.; Bai, Y. Experimental investigation on the mechanical and fracture evaluation of carbon Fiber-Reinforced cementitious composites with Nano-Calcium carbonate. *Constr. Build. Mater.* **2021**, *308*, 125095. [CrossRef]
23. Medljy, J.; El-Hassan, H.; El-Maaddawy, T. Effect of Recycled Aggregate and Steel Fibers on the Mechanical Properties of Alkali-Activated Slag/Fly Ash Blended Concrete. *ACI Symp. Publ.* **2021**, *349*, 210–223. [CrossRef]
24. El-Hassan, H.; Elkholy, S. Enhancing the performance of Alkali-Activated Slag-Fly ash blended concrete through hybrid steel fiber reinforcement. *Constr. Build. Mater.* **2021**, *311*, 125313. [CrossRef]
25. El-Hassan, H.; Elkholy, S. Performance Evaluation and Microstructure Characterization of Steel Fiber–Reinforced Alkali-Activated Slag Concrete Incorporating Fly Ash. *J. Mater. Civ. Eng.* **2019**, *31*, 04019223. [CrossRef]
26. Ravichandran, G.; Sivaraja, M.; Jegan, M.; Harihanandh, M.; Krishnaraja, A.R. Performance of Glass Fiber Reinforced Geopolymer Concrete under Varying Temperature Effect. *Int. J. Civ. Eng. Technol.* **2018**, *9*, 1316–1323.
27. Sathanandam, T.; Awoyera, P.; Vijayan, V.; Sathishkumar, K. Low carbon building: Experimental insight on the use of fly ash and glass fibre for making geopolymer concrete. *Sustain. Environ. Res.* **2017**, *27*, 146–153. [CrossRef]
28. Kumar, S.; Kumar, R.; Mehrotra, S.P. Influence of granulated blast furnace slag on the reaction, structure and properties of fly ash based geopolymer. *J. Mater. Sci.* **2010**, *45*, 607–615. [CrossRef]
29. Lakshmi, K.; Rao, M.S.N. Experimental Study on Geopolymer Concrete by using Glass Fibers. *Int. Res. J. Eng. Technol.* **2019**, *6*, 1693–1698.
30. Vijai, K.; Kumutha, R.; Vishnuram, B.G. Properties of Glass Fibre Reinforced Geopolymer Concrete Composites. *Asian J. Civ. Eng. Build. Hous.* **2012**, *13*, 511–520.
31. *ASTM C136/C136M-19*; Standard Test Method for Sieve Analysis of Fine and Coarse Aggregates. ASTM International: West Conshohocken, PA, USA, 2019.
32. *ASTM C127-15*; Standard Test Method for Relative Density (Specific Gravity) and Absorption of Coarse Aggregate. ASTM International: West Conshohocken, PA, USA, 2016.
33. *ASTM C29/C29M*; Standard Test Method for Bulk Density ('Unit Weight') and Voids in Aggregate. ASTM International: West Conshohocken, PA, USA, 2017.
34. *ASTM C131-06*; Standard Test Method for Resistance to Degradation of Small-Size Coarse Aggregate by Abrasion and Impact in the Los Angeles Machine. ASTM International: West Conshohocken, PA, USA, 2006.
35. Aliabdo, A.A.; Abd Elmoaty, A.E.M.; Salem, H.A. Effect of water addition, plasticizer and alkaline solution constitution on fly ash based geopolymer concrete performance. *Constr. Build. Mater.* **2016**, *121*, 694–703. [CrossRef]
36. El-Hassan, H.; Ismail, N. Effect of process parameters on the performance of fly ash/GGBS blended geopolymer composites. *J. Sustain. Cem. Mater.* **2017**, *7*, 122–140. [CrossRef]
37. Reforcetech. 2022. Available online: https://reforcetech.com/ (accessed on 18 February 2022).
38. Patankar, S.V.; Jamkar, S.S.; Ghugal, Y.M. Effect of Water-to-Geopolymer Binder Ratio on the Production of Fly ash Based Geopolymer Concrete. *Int. J. Adv. Technol. Civ. Eng.* **2012**, *4*, 15. [CrossRef]
39. Vitola, L.; Pundiene, I.; Pranckeviciene, J.; Bajare, D. The Impact of the Amount of Water Used in Activation Solution and the Initial Temperature of Paste on the Rheological Behaviour and Structural Evolution of Metakaolin-Based Geopolymer Pastes. *Sustainability* **2020**, *12*, 8216. [CrossRef]
40. Xie, J.; Kayali, O. Effect of Water Content on the Development of Fly Ash- based Geopolymers in Heat and Ambient Curing Conditions. *Constr. Build. Mater.* **2014**, *67*, 20–28. [CrossRef]
41. Zuaiter, M.; El-Hassan, H.; El-Ariss, B.; El-Maaddawy, T. Early-age properties of slag-fly ash blended geopolymer concrete reinforced with glass fibers—A preliminary study. In Proceedings of the 7th World Congress on Civil, Structural, and Environmental Engineering (CSEE'22), Virtual Conference, 10–12 April 2022.
42. *ASTM C143/C143M—10*; Standard Test Method for Slump of Hydraulic-Cement Concrete. ASTM International: West Conshohocken, PA, USA, 2010. [CrossRef]
43. *ASTM C138/C138*; Standard Test Method for Density (Unit Weight), Yield, and Air Content (Gravimetric) of Concrete. ASTM International: West Conshohocken, PA, USA, 2017. [CrossRef]
44. *ASTM C642*; Standard Test Method for Density, Absorption, and Voids in Hardened Concrete. ASTM International: West Conshohocken, PA, USA, 2013.
45. *BS 1881 Part:103*; Testing Concrete. Part 103. Method for Determination of Compacting Factor. British Standards Institution: London, UK, 1993.
46. *BS EN 12350–1*; Testing Fresh Concrete. Sampling and Common Apparatus. British Standards Institution: London, UK, 2019.
47. *BS EN 12390–3*; Testing Hardened Concrete. Compressive Strength of Test Specimens. British Standards Institution: London, UK, 2009.
48. *ASTM C39*; Standard Test Method for Compressive Strength of Cylindrical Concrete Specimens. ASTM International: West Conshohocken, PA, USA, 2015.
49. *ASTM C469*; Standard Test Method for Static Modulus of Elasticity and Poisson's Ratio of Concrete in Compression. ASTM International: West Conshohocken, PA, USA, 2014.
50. *ASTM C496*; Standard Test Method for Splitting Tensile Strength of Cylindrical Concrete Specimens. ASTM International: West Conshohocken, PA, USA, 2011.

51. *ASTM C1585*; Standard Test Method for Measurement of Rate of Absorption of Water by Hydraulic-Cement Concretes. ASTM International: West Conshohocken, PA, USA, 2013.
52. Mehta, P.K.; Monteiro, P.J.M. *Concrete: Microstructure, Properties, and Materials*, 3rd ed.; McGraw-Hill: New York, NY, USA, 2006.
53. *C1747*; Standard Test Method for Determining Potential Resistance to Degradation of Pervious Concrete by Impact and Abrasion. ASTM International: West Conshohocken, PA, USA, 2013.
54. *C597-02*; Standard Test Method for Pulse Velocity Through Concrete. ASTM International: West Conshohocken, PA, USA, 2003.
55. Saral, J.A.; Gayathri, S.; Tamilselvi, M.; Raj, B.R. An Experimental Study on Fibre Reinforced Geopolymer Concrete Composites-Glass Fibre, Copper Slag. *Int. J. Eng. Technol.* **2018**, *7*, 433–435. [CrossRef]
56. Nematollahi, B.; Sanjayan, J.; Chai, J.X.H.; Lu, T.M. Properties of Fresh and Hardened Glass Fiber Reinforced Fly Ash Based Geopolymer Concrete. *Key Eng. Mater.* **2013**, *594–595*, 629–633. [CrossRef]
57. Hu, C.-F.; Li, L.; Li, Z. Effect of fiber factor on the workability and mechanical properties of polyethylene fiber-reinforced high toughness geopolymers. *Ceram. Int.* **2021**, *48*, 10458–10471. [CrossRef]
58. De Figueiredo, A.D.; Ceccato, M.R. Workability Analysis of Steel Fiber Reinforced Concrete Using Slump and Ve-Be Test. *Mater. Res.* **2015**, *18*, 1284–1290. [CrossRef]
59. Kachouh, N.; El-Hassan, H.; El Maaddawy, T. Effect of steel fibers on the performance of concrete made with recycled concrete aggregates and dune sand. *Constr. Build. Mater.* **2019**, *213*, 348–359. [CrossRef]
60. Larsen, I.L.; Thorstensen, R.T. The influence of steel fibres on compressive and tensile strength of ultra high performance concrete: A review. *Constr. Build. Mater.* **2020**, *256*, 119459. [CrossRef]
61. Ismail, N.; El-Hassan, H. Development and Characterization of Fly Ash–Slag Blended Geopolymer Mortar and Lightweight Concrete. *J. Mater. Civ. Eng.* **2018**, *30*, 04018029. [CrossRef]
62. Giridh, M.G.; Shetty, K.K.; Nayak, G. Synthesis of Fly-ash and Slag Based Geopolymer Concrete for Rigid Pavement. *Mater. Today Proc.* **2022**, *60*, 46–54. [CrossRef]
63. Poornima, N.; Katyal, D.; Revathi, T.; Sivasakthi, M.; Jeyalakshmi, R. Effect of curing on mechanical strength and microstructure of fly ash blend GGBS geopolymer, Portland cement mortar and its behavior at elevated temperature. *Mater. Today Proc.* **2021**, *47*, 863–870. [CrossRef]
64. Yip, C.K.; Lukey, G.C.; Van Deventer, J.S.J. The coexistence of geopolymeric gel and calcium silicate hydrate at the early stage of alkaline activation. *Cem. Concr. Res.* **2005**, *35*, 1688–1697. [CrossRef]
65. El-Hassan, H.; Medljy, J.; El-Maaddawy, T. Properties of Steel Fiber-Reinforced Alkali-Activated Slag Concrete Made with Recycled Concrete Aggregates and Dune Sand. *Sustainability* **2021**, *13*, 8017. [CrossRef]
66. El-Hassan, H.; Hussein, A.; Medljy, J.; El-Maaddawy, T. Performance of Steel Fiber-Reinforced Alkali-Activated Slag-Fly Ash Blended Concrete Incorporating Recycled Concrete Aggregates and Dune Sand. *Buildings* **2021**, *11*, 327. [CrossRef]
67. Ganesan, V.; Ambily, P.S.; Ravi, R. Specimen Size Effect on Ultra High Strength Geopolymer Concrete (UHSGC). *Int. J. Eng. Res.* **2015**, *3*, 5.
68. Bhargava, P.; Sharma, U.K.; Kaushik, S.K. Compressive Stress-Strain Behavior of Small Scale Steel Fibre Reinforced High Strength Concrete Cylinders. *J. Adv. Concr. Technol.* **2006**, *4*, 109–121. [CrossRef]
69. Liao, W.-C.; Perceka, W.; Liu, E.-J. Compressive Stress-Strain Relationship of High Strength Steel Fiber Reinforced Concrete. *J. Adv. Concr. Technol.* **2015**, *13*, 379–392. [CrossRef]
70. Yuan, X.; Guan, H.; Shi, Y. Stress-Strain Relationship of Steel Fiber Reinforced Alkali Activated Slag Concrete under Static Compression. *Adv. Civ. Eng.* **2021**, *2021*, 7951646. [CrossRef]
71. *ACI 318-19*; Building code requirements for structural concrete (ACI 318-19): An ACI standard and commentary on building code requirements for structural concrete. American Concrete Institute: Farmington Hills, MI, USA, 2014.
72. Comité Euro-International du Béton. *CEB-FIB Model Code 1990 Design Code*; Thomas Telford, Ltd.: London, UK, 1993.
73. *AS3600*; Concrete Structures. Standards Australia: Sydney, Australia, 2009.
74. Park, S.H.; Kim, D.J.; Ryu, G.S.; Koh, K.T. Tensile behavior of Ultra High Performance Hybrid Fiber Reinforced Concrete. *Cem. Concr. Compos.* **2012**, *34*, 172–184. [CrossRef]
75. Chen, K.; Wu, D.; Xia, L.; Cai, Q.; Zhang, Z. Geopolymer concrete durability subjected to aggressive environments—A review of influence factors and comparison with ordinary Portland cement. *Constr. Build. Mater.* **2021**, *279*, 122496. [CrossRef]
76. Ali, B.; Qureshi, L.A.; Shah, S.H.A.; Rehman, S.U.; Hussain, I.; Iqbal, M. A step towards durable, ductile and sustainable concrete: Simultaneous incorporation of recycled aggregates, glass fiber and fly ash. *Constr. Build. Mater.* **2020**, *251*, 118980. [CrossRef]
77. Kwan, W.H.; Cheah, C.B.; Ramli, M.; Chang, K.Y. Alkali-resistant glass fiber reinforced high strength concrete in simulated aggressive environment. *Mater. Constr.* **2018**, *68*, 147. [CrossRef]
78. Ghosh, R.; Sagar, S.P.; Kumar, A.; Gupta, S.K.; Kumar, S. Estimation of geopolymer concrete strength from ultrasonic pulse velocity (UPV) using high power pulser. *J. Build. Eng.* **2018**, *16*, 39–44. [CrossRef]
79. *BS 1881 Part:203*; Specification for Testing Concrete.: Recommendations for Measurement of Velocity of Ultrasonic Pulses in Concrete. British Standards Institution: London, UK, 1986.